The impact of glauconite on petrophysical well logs in the Breda Subgroup and Oosterhout Formation

Ole de Keijzer

10 April 2025

Internship report – 10 April 2025

The impact of glauconite on petrophysical well logs in the Breda Subgroup and Oosterhout Formation

Ole de Keijzer

Author	Ole de Keijzer (6398383) E-mail: oledekeijzer@gmail.com	
University	Utrecht University	
Master program	Earth Structure and Dynamics (track: Earth Materials)	
Internship period	01-11-2024 – 11-04-2025	
Internship Organisation	TNO-GDN, Department Hydrology and Resevoir Engineering	
TNO supervisors	Lies Peters	E-mail: lies.peters@tno.nl
	Angela Pascarella	E-mail: angela.pascarella@tno.nl
UU supervisors	Sonja Geilert	E-mail: s.geilert@uu.nl
	Leo Kriegsman	E-mail: leo.kriegsman@naturalis.nl
Word count	19137	

Contents

Summary

Petrophysical well logs are useful tools to study the lithology and characteristics of the subsurface. The gamma ray (GR) log is often used to calculate the volume of shale (Vshale) of a lithology, which can be used for porosity and permeability calculations and the identification of aquifers. However, in the Oosterhout Formation and the Breda Subgroup of the Upper North Sea Group in the Netherlands, high GR values, normally associated with shales, are measured in permeable glauconitic sands. This results in challenges for the interpretation of the GR log and additional risks if these reservoirs are used for medium deep geothermal energy and aquifer thermal energy storage. Therefore, this study focuses on the distribution and occurrence of glauconitic sands and their effect on GR and other well logs. Lithological and petrophysical data, mainly GR, spectral gamma ray (SGR) and spontaneous potential (SP), of shallow and deep wells in certain focus areas were evaluated and compared. Cutting from deep wells were analysed to increase the lithological data in the research areas. To be able to locate glauconite-rich lithologies, the glauconite content in different wells is mapped and the relationship between thorium/potassium (Th/K) ratio and glauconite content is tested as an identification method for glauconitic lithologies. Moreover, alternative well logging methods, such as SP and SGR are tested as possible alternative methods for the Vshale calculation and the interpretation of well log data in problematic lithologies. It is concluded that the glauconite content varies a lot, both laterally and vertically. In the studied wells, three glauconite peaks were recognized, occurring in the Tilburg Member of the Oosterhout Formation, the Diessen Formation in the Breda Subgroup and the Groote Heide Formation in the Breda Subgroup. The SGR definitely helps to identify glauconite rich lithologies that correspond to peaks in potassium content, but does not provide a precise way to quantify the glauconite content with the thorium-potassium ratio, as the uncertainty is too large. While glauconite certainly has a significant effect on the Gamma Ray log, it is not the only contributor to the elevated GR values in the Oosterhout Fm and Breda Sg and increased uranium and thorium contents, especially around unconformities, should also be taken into account. When petrophysical analysis is used to determine the lithology and shale volume, the Th log from the SGR log and the SP log are very useful to calibrate the GR log and can help improve the petrophysical interpretation methods.

1 Introduction

1.1 Problem statement

In the process of creating a more sustainable heat network in the Netherlands, geothermal energy is an important heat source (Peters et al. 2022). Therefore, a lot of focus is given to investigating the potential of geothermal energy in the Netherlands. At first, the geothermal industry has been focussing on deep (>1500m) and warm reservoirs in the Dutch subsurface. However, medium deep interval, referring to 200-1500m depth, has a large potential as well, especially in the Roer Valley Graben (RVG) and the Zuiderzee Low (ZZL) area (Smit 2022; Veldkamp et al. 2023). Moreover, this medium depth interval is the main focus for high temperature aquifer thermal energy storage (ATES) (Vrijlandt et al. 2023). Therefore, one of the goals of the project "Warming^{UP} Geothermal and Storage Upscaling" (Warming^{UP}*GOO*) is to increase the knowledge and insight of this medium deep interval of the subsurface to minimise the risks of geothermal energy extraction and ATES (Houben et al. 2023).

The Oosterhout and former Breda Formation (Fm), nowadays called the Breda Subgroup (Sg) and separated in the Diessen Fm and Groote Heide Fm (Munsterman et al. 2025), take up a significant part of this medium depth interval. These formations contain shaly and sandy parts, which vary in thickness and depth throughout the Netherlands. Depending on the sequence, thickness and depth of the different lithologies, the formations can be useful reservoirs for geothermal and ATES purposes at certain locations (Smit 2022).

The geological models that are used to map these units are based on limited data on locations where the formations fall within the medium deep interval. Seismic subsurface data and data from deep wells can improve the geological models in the medium deep interval. The petrophysical well logs from deep wells are very important to link the seismic data of the relatively deeper parts to the lithological data in the shallower parts (Houben et al. 2023). Especially when the sampling frequency during drilling is low due to economic and technical reasons, petrophysical well logs provide more continuous information that can help to identify differences in for instance lithology and groundwater salinity (Serra 1984). One commonly used petrophysical well log, the gamma ray (GR) log, can be used to calculate the shale volume (Vshale) of the wall rock and thus identify potential reservoirs. However, specific accessory minerals occurring in sands, such as feldspars, micas and glauconite, can create a shale-like signal in the GR log, creating difficulties in the interpretation and erroneous results when the standard calculations for Vshale are applied (Rider 2002).

The mineral glauconite is one of these minerals that can result in problematic well log interpretation. Chemically glauconite behaves as a clay mineral and contains water and clay-like chemical components, but in contrast to other clay minerals, the occurrence of glauconite is usually as 'fine sand'-sized grains (Abouzaid et al. 2016). The mineral is typically common in the sands of the Oosterhout Fm and Breda Sg and shale-like GR signals are measured in the (glauconitic) sands of these formations. Without any adjustment to the interpretation methods of a Vshale that are often used, the permeable glauconitic sands have the risk to be interpreted as impermeable shales, especially when the glauconite content within a formation is not constant.

Apart from the problems with well log interpretation, glauconite creates mechanical problems for well drilling and pile driving operations (Piedrabuena 2024; Westgate et al. 2023). Under compaction circumstances, the mineral is crushed and forms a clayey pseudomatrix that occludes the borehole as well as the porosity of the wall rock (Diaz et al. 2002; Piedrabuena 2024; Van Alboom et al. 2012; VANCAMP 2011). Moreover, special precautions should be taken into account when using groundwater from a glauconitic sand reservoir, as the porewater present in glauconitic sands is always enriched in iron (Van Alboom et al. 2012).

The challenges in the interpretation of the well logs make the characterisation of the formations more difficult and together with the mechanical problems, these increase the financial risks when these reservoirs will be used for geothermal or ATES purposes. Therefore, a better understanding is needed of the distribution and occurrence of the glauconite in the Oosterhout Fm and Breda Sg, as well as the effect of the mineral has on the GR log and other petrophysical well logging methods.

1.2 Objective and Research questions

The objective of this research is to better understand the presence and impact of glauconite on well logs and consequently improve the well log interpretation in the Oosterhout Fm and Breda Sg. The following research questions are formulated:

- What is the presence and distribution of glauconite in the Oosterhout Formation and Breda Subgroup of the Upper North Sea group in the research areas?
- Can glauconitic lithologies be identified using spectral gamma ray logs?
- How large is the impact of glauconite on the gamma ray log?
- Which alternative methods or corrections for the effect of glauconite can improve the interpretation of petrophysical well logs?

To answer these questions, subsurface data from all over the Netherlands and Belgium will be used and analysed. However, the focus will be on two specific research areas, mainly to confine the research on the presence and distribution of glauconite. The first research area is Southern Flevoland and the Gelderse Vallei, both part of the ZZL. This area, in this report called the Zuiderzee Region (ZZR), is chosen because it is one of the target areas of the Warming^{UP}*GOO* project and has a high potential for geothermal and ATES in the Breda Sg and Oosterhout Fm. The ZZR, however, has little data on the Breda Sg and Oosterhout Fm that are quite deep in this region. Therefore, the second research area is the western part of the province Noord-Brabant, in this report called the West-Brabant Region (WBR), because in this area the amount of data in the Breda Sg and Oosterhout Fm is higher and can serve as an analogue for the ZZR. The data is available through literature and multiple data portals, such as Dinoloket (TNO-GDN 2025a) and NLOG (TNO-GDN 2025b), and by analysis of drilled cuttings from wells stored at the Core Shed (Kernhuis) in Zeist.

The results of this research are meant to provide more information on the impact of glauconite on well log interpretation and help prevent lithological misinterpretation in the future. This research will subsequently contribute to the Warming^{UP}*GOO* project and help to minimise the risks of geothermal energy extraction and ATES in the transition to a more sustainable heat network.

2 Background information

2.1 Glauconite

Glauconite is known for its typical colour ranging from olive green, black green to blue green. The mineral has a hardness of 2 on Mohs scale (Abouzaid et al. 2016). The average density is 2.86 g/cm^3, which is significantly higher than the density of quartz sand, 2.64 g/cm^3 (Schlumberger 2013). Sands with a high percentage of glauconitic grains are also known as greensands (Patchett et al. 1993). Next to the commonly known form of rounded grains or pellets, glauconite can also be found as filled fossil casts of foraminifers, altered mica flakes or in some rare cases as a grain coating (Odin and Matter 1981; Thomas et al. 2003). In the research of Adriaens et al. (2014), it is shown that glauconite in the Belgian subsurface can also occur as clay and silt-sized particles, due to transport and abrasion of the more commonly found sand-size pellets.

The term glauconite, referring to a clay mineral occurring in greenish grains or pellets in shallow marine sediments, has long been ill-defined and led to confusion (Huff 1990). Odin and Matter (1981) proposed the facies term 'glaucony' to describe the material of the greenish grains, with glauconitic smectite and glauconitic mica as end-members of the glauconitic mineral family. The glauconitic mica mainly forms by the crystal growth and recrystallisation of (glauconitic) smectite (Odin and Matter 1981). This glauconitic mica end-member is described and defined by the International Mineralogical Association (IMA) as "glauconite", a dioctahedral interlayer-deficient mica. This indicates that it consists of layers with one tetrahedral between two octahedral sheets, separated by interlayer cations with a charge in the range 0.6-0.85, and has less than 2.5 octahedral cations per formula unit (Rieder et al. 1998). The chemical formula of glauconite is $(K, Na)(Fe, Al, Mg)_2(Si, Al)_4O_{10}(OH)_2$, which indicates that glauconite is a mineral series with variations in K^+, Na^+, Fe^{3+}, Fe^{2+}, Al^{3+}, Mg^{2+} and Si^{4+} content (Rieder et al. 1998; Drits et al. 2010).

The evolution of glaucony minerals from an Fe^{3+}-rich smectite to a glauconite mica is also called glauconite evolution or glauconitisation. During the glauconitisation, the chemistry and appearance of the glaucony minerals slowly changes, and the sodium (Na^+) is replaced by potassium (K^+). The latest insights show that glauconite crystallisation at the expense of smectite occurs by a layer-growth mechanism, where an increase in Fe^{3+}/Fe^{2+} is stabilized by the increase in K^+ (López-Quirós et al. 2020), but this incorporation of (K^+) is paralleled by and enrichment in magnesium (Mg^{2+}) silicon (Si^{4+}) and aluminium (Al^{3+}) in carbonate rocks (Amorosi et al. 2007). Glauconitisation can be subdivided into the four stages described by Odin and Matter (1981), Obasi et al. (2011) and Piedrabuena (2024):

1. **Nascent glauconitic smectite:** The initial substrate still has a simple pellet shape and a receives a light green colour, as the first iron and potassium rich glauconitic crystals grow. The K^+-content is very low (ca. 2-3%), but slowly increases during this stage as organic matter and Al-content decreases and the mineral becomes softer.
2. **Slightly evolved glauconite:** As the iron- and potassium-content increase and amount of organic matter increases, the colour gets darker and streaks of glauconite form within the substrate. The K^+-content is grows from 3% to 5% in this stage.
3. **Evolved glauconite:** Cracks start to form in the grain, allowing potassium to reach to the centre of the grain. The organic matter is completely gone and the amount of iron increases more slowly, but the K^+-content increases from 5% to 7%. The grain is darkening further in this stage.
4. **Highly evolved glauconite:** The increase K^+-content continues and reaches levels up to 8%, The colour goes from dark green to black and the particle gets more spherical, resulting from a crust of slightly-evolved glauconite around the grains. The highly evolved glauconitic mica has reached a form that will remain stable after burial or further exposure at the sediment-water interface.

This evolution process, visualised in Figure 2-1, takes 1 My, depending on the circumstances such as temperature, cation supply, burial rate and depositional environment (Baldermann et al. 2013). Glauconitisation takes place at the sediment-water interface and therefore only occurs when the sedimentation rate is low, as the evolution will stop when the glauconite grains get buried too deep and are out of reach for the cations from the seawater (López-Quirós et al. 2019; Piedrabuena 2024).

Due to its specific and time-consuming evolution process, Glauconite can be a useful mineral for determining the palaeoenvironment, as glauconitisation occurs mostly in microenvironments of reduction in marine nearshore sediments (Huff 1990; Abouzaid et al. 2016). The glauconitic facies is associated with very low sedimentation rates in transgressive sequences (Li et al. 2012). Moreover, glauconite can help to determine the age of the sediments when it is used for K-Ar dating (Vandenberghe et al. 2014).

The low hardness value and clay-like characteristics of glauconite create problems when stress is applied to a glauconitic sand. The glauconite grains, with a hardness of 2 on Mohs scale, break much more easily than the quartz grains with a hardness of 7 (Piedrabuena 2024; VANCAMP 2011). The crushed glauconite then forms a clayey pseudomatrix that occludes the primary porosity and reduces the permeability. This can be the result of compaction and burial processes (Diaz et al. 2002; Van Alboom et al. 2012), but also of human activities such as pile driving and borehole drilling (Westgate et al. 2023; van Staveren and de Wit 1995).

Due to its potassium content, glauconite can have a significant effect on the gamma ray log. The iron in the glauconite effects density and NMR logs and the hydrogen in the mineral effect neutron logs. The resistivity logs can be effected as well, because of the clay-like high cation exchange capacity of the glauconitic minerals (Rider 2002).

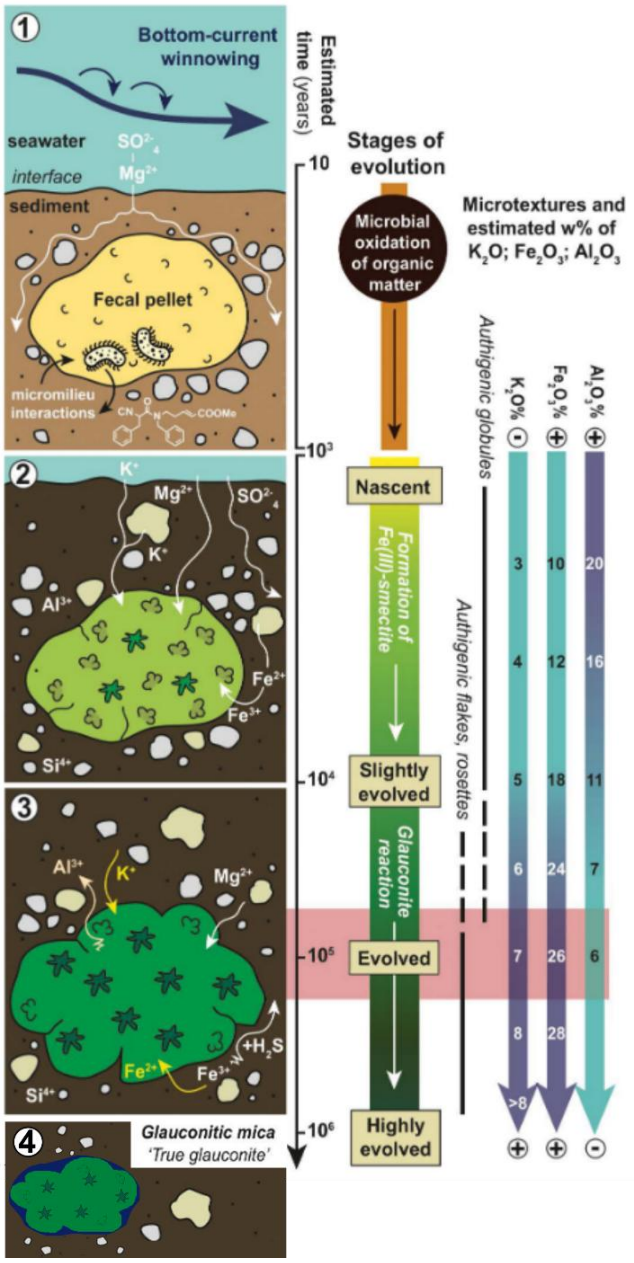

Figure 2-1: Glauconite evolution. The drawings 1, 2, 3 and 4 show the glauconite grain is the first three phases and the chemical interaction with the subsurface. The arrows on the right show the evolutionary progress over time with the expected element content of the mineral. Figure is derived from López-Quirós et al. (2020) and altered to include a drawing of the fourth 'highly evolved' stage in glauconite evolution.

2.2 Petrophysical well logging methods

The Petrophysics of rock formations concern the physical properties of the rock and the fluids it contains. Petrophysical information is often derived by petrophysical logging tools providing well logs. Each petrophysical log contains its own specific information and, often combined with each other, they can be used to indicate parameters such as sand/mud ratio, porosity, permeability and hydrocarbon saturation. The petrophysical and other geophysical logging tools are mounted on a sonde, a device that can be lowered down a borehole on a wireline while the geophysical instruments record the information of the different strata in the borehole wall (Nichols 2009). In this section, the most relevant petrophysical well logs are discussed for this research.

2.2.1 Gamma Ray and Spectral Gamma Ray

The Gamma Ray log (GR) records the natural radioactivity in the rocks, coming from the decay of potassium-40 (K), uranium-238 (U) and thorium-232 (Th) isotopes. The GR tool is a gamma ray detector that consists of a scintillation counter and a photo-multiplier. When gamma rays pass through the scintillation counter, typically a sodium iodide crystal with minor Thallium impurities, they cause a flash that is collected by the photo-multiplier. The accumulated energy over a set period of time from the received gamma rays is the measured gamma ray value, expressed with the API (American Petroleum Institute) unit (Rider 2002).
The GR signal can be used to distinguish between sandstones and shales (including all different types of mudrocks), because of their difference in natural radioactivity. Sandstone and limestone generally have a low natural radioactivity, while shale has a typically high natural radioactivity, mainly due to its high potassium content (Nichols 2009).

In addition to the effect of shale and clay, the Gamma Ray signal is also affected by accessory minerals that contain high amounts of K, U or Th. Some types of drilling fluid or mud contain K as well and therefore affect the measured gamma ray signal. Furthermore, the intensity of the measured GR is dependent on the size of the borehole, as this affects the distance between the wallrock and the GR tool.

The Spectral Gamma Ray (SGR) tool is similar to the normal GR tool, but has a greater volume and can therefore also measure the intensity of the gamma ray signal. This intensity or energy can be used to identify the radioactive element each gamma ray comes from, which all have their own distinctive energy peaks. The SGR log thus includes three separate logs that indicate the U and Th content in parts per million (ppm) and the K content in mass percentage. The SGR log can be used to derive a quantitative radioactive mineral volume and a more accurate shale volume and to qualitatively indicate dominant clay mineral types and fractions.

Each lithology or mineralogy has its own specific combination of radioactive elements. Shales are often enriched in all three radioactive elements, while sands and calcium-rich lithologies are depleted in all three. Mica's, Feldspars and Glauconite minerals are mostly enriched in K, but less enriched in Th and U. Organic material is much more enriched in U than in K and Th and each clay mineral also has its own specific proportions of radioactive elements, as is visible in Figure 2-2a and Table 2-1, Moreover, the ratio between K and Th is commonly used as an indication of the mineralogy in a sample, visualised with a Th-K mineral map (Figure 2-2b). While this mineral map is a useful tool. It should be noted that it shows the K-Th ratios typical for end-member minerals, meaning that a sediment containing 40% kaolinite and 40% glauconite does not necessarily plot in either of those mineral fields, but rather somewhere om between.

The intensity of the GR signal is different for each radioactive element. Th and U are normally present in much smaller amount than K, but 2 ppm of U results in a similar GR response as 1% of K (Rider 2002). The commonly used multipliers that relate elemental content to GR in API units are shown in Table 2-2

Table 2-1: Potassium and thorium content of different minerals.

Mineral	K content (%)	Th content (ppm)
Illite	3.5 - 8.3 (Rider 2002)	6 – 22 (Rider 2002)
Kaolinite	0 - 1.5 (Rider 2002)	18 – 26 (Rider 2002)
Smectite	0 - 0.6 (Rider 2002)	10 – 24 (Rider 2002)
Little-evolved glauconite	4 – 6 (Odin and Matter 1981)	2 – 8 (Rider 2002)
Evolved glauconite	6 – 8 (Odin and Matter 1981)	2 – 8 (Rider 2002)
Highly evolved glauconite	8 – 10 (Odin and Matter 1981)	2 – 8 (Rider 2002)
Muscovite	9.8 (Rieder et al. 1998)	6 – 22 (Rider 2002)
Average clay	2 - 3.5 (Rider 2002)	8 – 18 (Rider 2002)

Table 2-2: The different GR responses for a specific amount of each radioactive element Th, U and K (Rider 2002).

Radioactive element	Content	GR response
U	1 ppm	8.09 API
Th	1 ppm	3.93 API
K	1 %	16.32 API

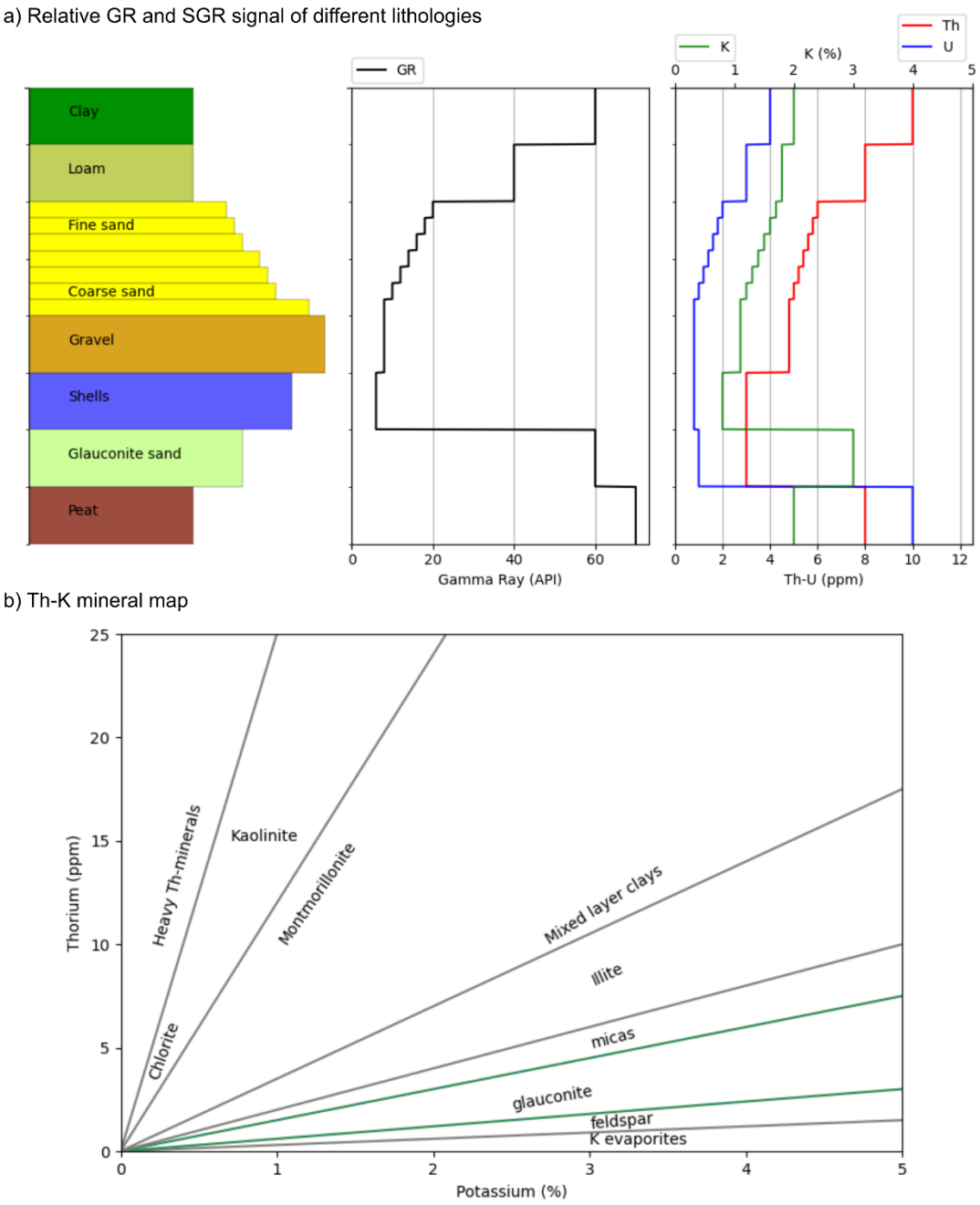

Figure 2-2: a) Typical relative GR and SGR signals for different lithologies. Note that these are relative theoretical end-member values and can vary due to the size of the borehole or minor varieties in lithology. b) Th-K mineral map, showing the typical Th and K content of various minerals. These figures were created using information from Rider (2002).

2.2.2 Volume of Shale

The GR log is often used to quantify the volume of shale or clay (both referred to as Vshale in this report) of a lithological interval. This is done by determining the GR signal that is typical for a 100% shale and a 100% clean sand, and using these as cutoffs to scale the GR log so that it indicates the volume of shale/clay as a percentage. While there is no scientific basis for assuming a linear relationship between the GR signal and the Vshale, there is a scientific basis to assume that clay minerals have higher GR signal, due to their K and Th content. This method works out quite well in most cases, when there are not much accessory minerals present that are not accounted for in this method. Moreover, it should be taken into account that the GR log reflects the radioactivity of clay-minerals, while the volume of shale/clay is used as a measure of the amount of clay-sized sediments, which is not necessarily the same (Rider 2002).

The Vshale is usually determined for each formation separately. This is done by determining the cutoff values for each formation and therefore taken into account the formations characteristics and minimizing the effects of background mineralogy.
The Vshale can also be derived in a similar way using the individual elemental contributions of the SGR log and other petrophysical well logs like the spontaneous potential (SP) and neutron-density (ND).

2.2.3 Resistivity

Resistivity logs are generated by a variety of logging tools that measure either the electrical resistivity directly or derive the resistivity from the electrical conductivity of the rocks and their pore fluids. The results can be used for a number of purposes, such as indicating changes in salinity of the pore fluid, the presence of clay minerals and shales, and the porosity and permeability (Nichols 2009).

The resistivity, measured in $\Omega \cdot \mathrm{m}$, is the resistance with normalized dimensions. The measured resistivity is dependent on several things. The electrical current mainly travels through formation fluid, so its conductivity is the primary factor in the resistivity logs. Saline pore water, for instance, is a better conductor than fresh water and therefore has lower resistivity values. The effect of the pore connections is expressed as the formation resistivity factor. This factor indicates how much the (non-conductive) rock matrix increases the resistivity by making the pathway of the current through the pores more complex.
For most rock types, the resistivity is simply a measurement of the pore fluid conductivity and the complexity of the pore connections. However, clay particles do not have a passive role in conducting, as the electrical current can travel through both the pore water and the clay itself. The silicate layers of a clay become negatively charged in the presence of water, making the surface of the clay mineral layers conductive. The conductivity varies for different clay species and is dependent on the surface area available in the clay mineral. This surface area is related to the cation exchange capacity of the clay mineral, which indicates its ability to exchange cations. The resistivity can thus also be an indication of the clay species. For the conductivity behaviour of clay-sand mixtures, the interpretation is rather complex and no general consensus is yet reached on the interactions between conductive clays and the conductive pore fluids. In general, with a lower pore fluid conductivity, the importance of the rock matrix conductivity is larger and more electrical current will go through the shales instead of the pore fluid (Rider 2002).

2.2.4 Spontaneous potential

The spontaneous potential (SP) log reflects the natural potential difference or voltage measured between electrodes in the well and at the earth's surface. The natural potential is created only when a pore fluid with different salinity is in contact with the borehole fluid and ions can move from the formation water to the borehole, creating currents. The Spontaneous potential, measured in millivolts (mV), is negative when the pore fluid is more saline than the borehole fluid and the resistivity of the pore fluid is lower. A positive value can indicate that the borehole fluid is more saline and has a lower resistivity than the pore fluid or that the lithology includes (negatively charged) shale layers. The SP log can be used to calculate the Vshale as well as the formation-water resistivity. The SP log can be used for the correlation with the GR by comparing the Vshale logs from both measurements. While the GR provides much more information and a better bed boundary definition, the overall patterns should be similar in most cases. While the SP is a cheap and useful tool, it requires an electrode on the earth surface. This makes SP measurements in offshore wells very difficult (Rider 2002).

2.2.5 Other Petrophysical well logs

A sonic log record the velocity of sound waves travelling through the formation. The sonic velocity can give an indication about the density of the lithology and, if the lithology is known, can be used to calculate the porosity (Nichols 2009).

The density log gives a record of the formations bulk density, which is indicative of its lithology and porosity. By emitting gamma radiation and measuring the amount of radiation that returns, this tool measures the electron density of the rocks. This electron density is in general almost identical to the bulk density of the rock, with the exception of the interference of water (Rider 2002).

The same logging tool acquires what is called the Photoelectric Factor log (PEF), which is another log recording the photoelectric absorption index (Pe). This index is mostly dependent on the atomic number of the rock components and is less effected by the porosity. Therefore the Pe can be used to identify the rock matrix and indicate the lithology and diagenetic minerals. (Rider 2002).

The neutron logging tool emits neutrons and then counts the number of returning neutrons by measuring the energy of the neutrons. As the neutrons collide with hydrogen nuclei, that have a similar size, they lose their energy. This ultimately is a measure of hydrogen concentration. Most of the hydrogen is present in the pore fluid, so the hydrogen concentration is in means a measure of porosity. However, clay minerals have hydrogen atoms in their mineral structure as well, which cause high neutron responses in clay-rich intervals (Nichols 2009). The neutron and density log (combined neutron-density or ND) can also be used to calculate and quantify the Vshale (Rider 2002)

The nuclear magnetic resonance log (NMR) measures the porosity and the pore-size distribution of a saturated formation. The tool produces a strong magnetic field to polarise the hydrogen nuclei and measured the relaxation time of the hydrogen nuclei when the magnetic field is switched of, which increases if nuclei are interacting with grain surfaces. Therefore, the NMR log shows how much of the pore fluid is close to the pore boundary, indicating the size of the pore space (Nichols 2009). For reservoir characterisation, the NMR tool can be very useful in lithologies that contain certain accessory minerals that affect other petrophysical well logs. The NMR is unaffected by most of these accessory minerals, but corrections are needed for iron-containing accessory minerals, such as glauconite (Abouzaid et al. 2016).

The caliper measures variations in borehole size. The tool pushes its arms against the borehole wall and measures the lateral movement of the arms. This technique can therefore identify borehole caving, indicating a shaly lithology, and mudcakes, indicating a permeable bed. More importantly the caliper functions as a quality control of other logs, as variations in borehole size can effect other petrophysical measurements (Rider 2002).

2.3 Geological background

The formations of interest, specifically the Oosterhout Fm and Breda Sg, are the lowermost stratigraphic units of the Upper North Sea group (NU), which includes the sediments from the Miocene period onward. The NU is located on top of the Middle North Sea Group (NM) or older formations and reaches depth up to 1500m (TNO-GDN 2025c).

2.3.1 The Oosterhout Formation

The Oosterhout Formation is a shallow marine deposition of very fine to very coarse sand. Locally, the beds in the Oosterhout Fm can contain clay, glauconite or shells. The lithological upper boundary of the formation is defined as a transition to the coarser, glauconite-poorer sands of the Maassluis Fm, a sharp contact with the coarser fluvial and coastal sands and gravels of the Kiezeloöliet, Waalre or Peize Fm, or a slow transition to aeolian and locally fluvial sands of the Strampoy Fm. The lithological lower boundary is the transition to the finer sands of the former Breda Fm, with a higher glauconite content and a lower shell content (TNO-GDN 2024b).

Three members are recognized within the Oosterhout Fm, according to the Stratigraphic Nomenclator of Dinoloket (TNO-GDN 2024b). In the southwest of the Netherlands, the Wouw Member (Mb), consisting of greyish clay layers, and the Sprundel Mb, consisting of layers with a high shell content, are identified. The Lievelde Mb is only found in the eastern part of the Netherlands and has white-grey fine sands which are well sorted, coarsening upwards and contain some glauconite. However, Munsterman et al. (2019) defines two other members at the base of the Oosterhout Fm, the Tilburg Mb and the Goirle Mb. They can be recognized by unique lithological characteristics as well as unique seismic facies and are present in the central and southern parts of Brabant. The Tilburg Mb consists of dark green-grey, highly glauconitic, slightly silty and clayey sands. The base of the Tilburg Mb is interpreted as a flooding surface and is recognized by a positive gamma ray excursion, with high gamma ray values for the whole member. The Goirle Mb, located on top of the Breda Sg and underneath the Tilburg Mb, is a section of light-grey to white fine sands and low fluctuating concentrations of glauconite.

The Oosterhout Fm is mainly of Pliocene age and is biostratigraphically recognized by Piacenzian and Zanclean fauna. Therefore the base of the Pleistocene and the Late Miocene Unconformity (LMU) can be seen as the upper and lower boundaries of the Oosterhout Fm, respectively. The chronostratigraphic and lithostratigraphic interpretations are however not always easy to combine, as the lithofacies development of the Oosterhout Fm and boundary Formations can be strongly diachronous (Houben 2025).

The Oosterhout Fm is present almost everywhere in the Dutch subsurface, with the exception of Limburg and the border regions in Zeeland, Gelderland and Overijssel (Figure 2-3). Its thickness can be up to almost 200m and its lower boundary reach depths of more than 500m. In the geohydrological model BRO REGIS II, the Oosterhout Fm is divided in three parts. From top to base, these are the Oosterhout clay layer, the Oosterhout sand layer and the Oosterhout complex layer, which is mostly a mixture of clays and sands.

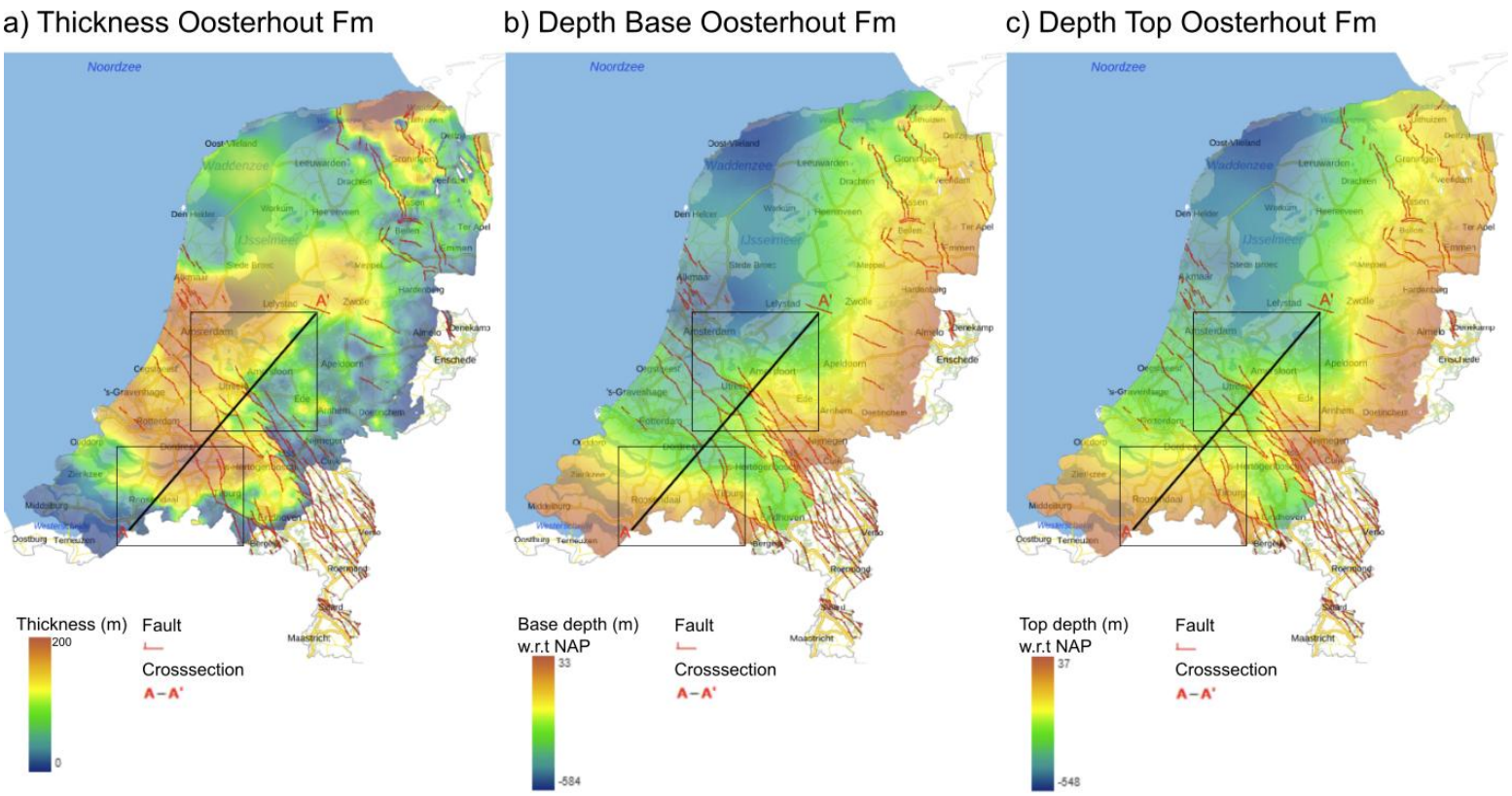

Figure 2-3: Thickness and depth maps of the Oosterhout Fm according to the model BRO DGMv2.2 on Dinoloket. The cross section from point A to A' indicated is shown in Figure 2-6.

2.3.2 The Breda Subgroup

The Breda Subgroup, formerly known as the Breda Formation, is also a shallow marine deposit, but with some continental lignite layers including near the margins of the unit. Overall the lithology is greyish to blackish green silty to medium fine sand and also clay. The deposits can be very glauconitic, calcareous, locally micaceous and organic as well. Goethite and Phosphorite concretions can also be found in some layers. The lithological upper boundary is a gradual transition to the less glauconitic, shell-rich sands and clays of the Oosterhout Fm described above or in the southeast a sharp and erosive contact with the terrestrial deposits of the Kiezeloöliet, Inden, Ville or Köln Fm. The lower boundary is marked by an unconformity which is visible as a gradual transition to the less glauconitic shallow marine and coastal sands of the Veldhoven Fm or a sharp contact with the marine clays of the Rupel Fm, Boom Mb, or older units (TNO-GDN 2024a).

Within the former Breda Fm, several members were recognised. The Delden, Zenderen, Eibergen, Aalten and Nieuweschans Mb are present in the northeastern part of the Netherlands, close to the German border. The Vrijherenberg, Heksenberg and Kakert Mb are recognised in the southeastern part of the Netherlands (mainly Limburg) and the Rucphen Mb in the southwestern part of the Netherlands(TNO-GDN 2024a).

The Breda Sg is of Oligocene to Early Pliocene, but mainly Miocene age and can be biostratigraphically bounded by the Late Miocene Unconformity (LMU) at the top and the Early Miocene unconformity (EMU) at the bottom. These unconformities can be recognised by changes in biostratigraphy and are visible in as seismic surfaces as well. In the GR log, the LMU is correlated to a gradual increase in GR signal with depth and the EMU is a correlated to a less gradual decrease in GR signal (Munsterman et al. 2019; Houben 2025). The new subdivision proposed by Munsterman et al. (2019) splits the Breda subgroup in the Groote Heide Formation and the Diessen Formation. Their division is marked by another unconformity, the Middle Miocene Unconformity (MMU). This unconformity has a very characteristic GR peak, and can be recognised with biostratigraphy and seismic interpretation as well.

Lithologically, the new formations share a lot of characteristics, but the different stratigaphic sequences have a few minor differences to tell the lithology apart. For instance, the Diessen Fm has traces of molluscs and sea urchin spines, a transition from grey-greenish clays and sandy loam at the base to silty fine-grained sand at the top and an sharp increase in epidote and amphibole, upwards followed by an increase in tourmaline and metamorphic minerals, while the Groote Heide Fm has grey to black green fine silty sands and clay and is typically even more enriched in glauconite.

The former Breda Fm is found in the whole country , with the exception of some border regions in Limburg, Zeeland, Gelderland and Overijssel (Figure 2-4). The Breda Fm can be up to 900m thick and its lower boundary can even reach depths of 1200m in the RVG. In the geohydrological model BRO REGIS II, the former Breda Fm was divided into the Breda sand and the Breda Clay. The sandy part of the Breda Fm is present in Zeeland, Noord-Brabant, Limburg and partially in Gelderland, Utrecht and Overijssel (Figure 2-5). The Breda sand is expected to be present in part of Flevoland as well, but this is not visualised in the REGIS model, due to the lack of data (Smit 2022).

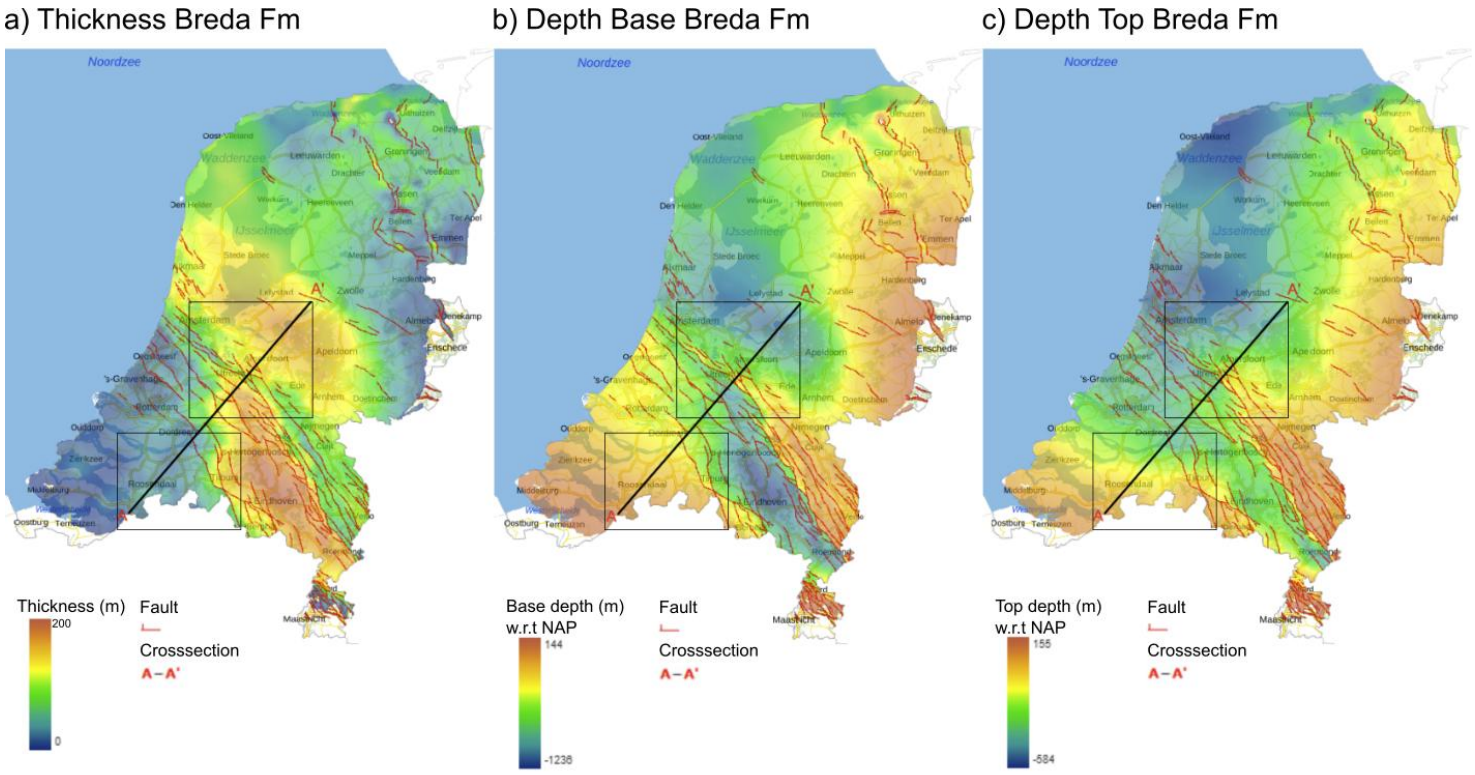

Figure 2-4: Thickness and depth maps of the former Breda Fm according to the model BRO DGMv2.2 on Dinoloket. The cross section from point A to A' indicated is shown in Figure 2-6.

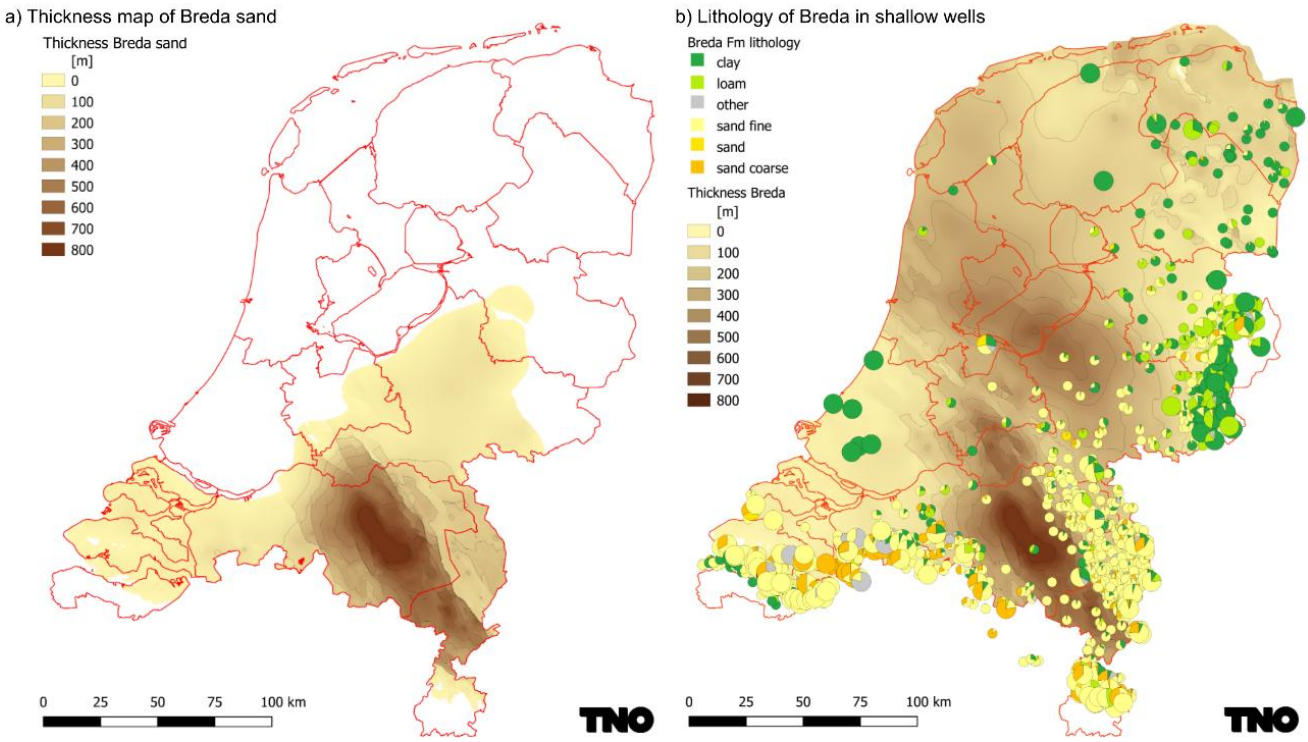

Figure 2-5: a) Map of sand thickness within the Breda Fm according to the model BRO REGIS II. B) Map of Breda Thickness displaying the lithology of the Breda Fm in all shallow wells. Both images derived from Smit (2022).

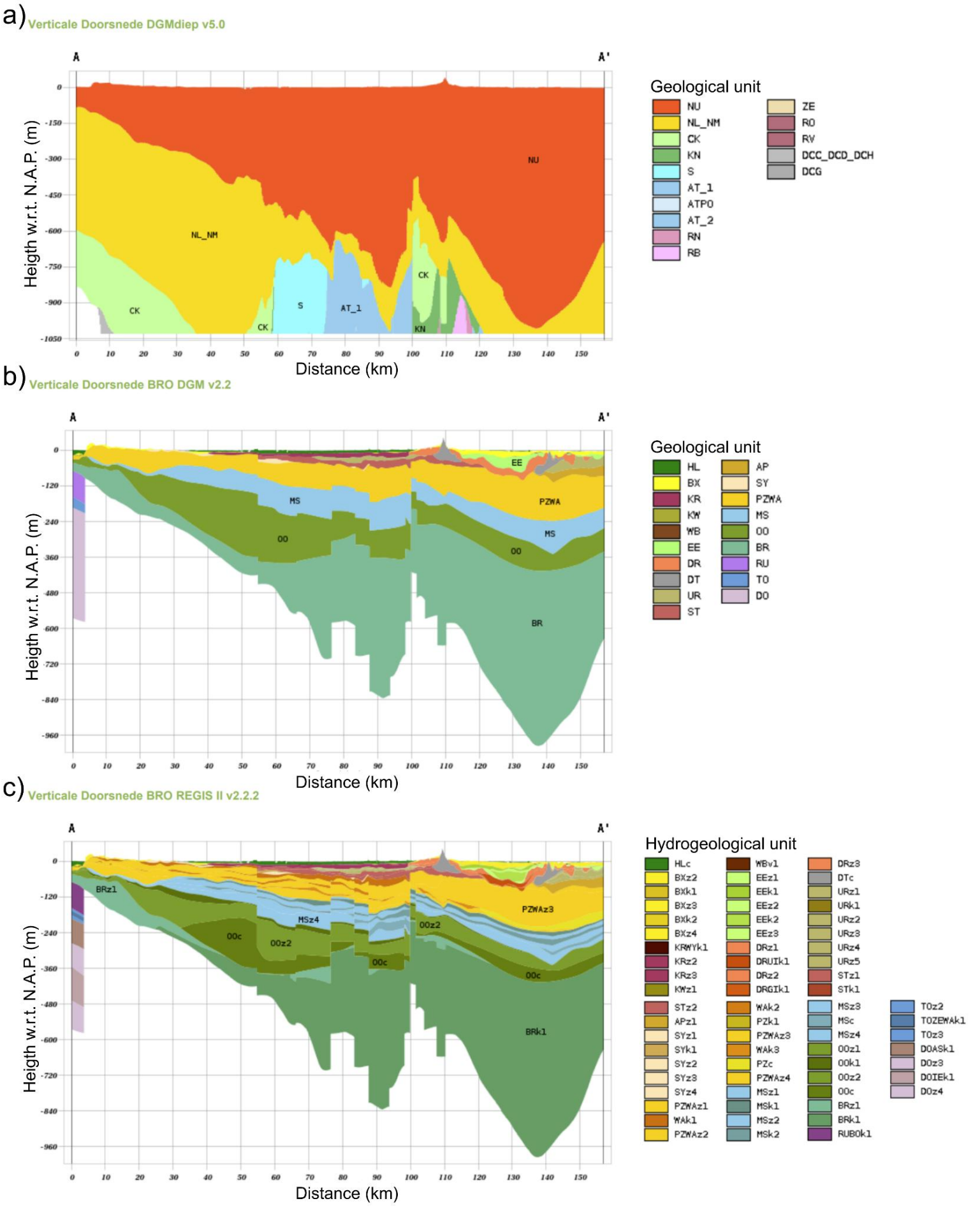

Figure 2-6: 2D cross-sections through both research areas with three different models from Dinoloket (TNO-GDN 2025a). The cross section line is indicated on the maps of Figure 2-3 and Figure 2-4. a) Model DGMdiep showing all larger geological groups. b) Model BRO DGM showing all formations of the Upper North Sea Group. c) Model BRO REGIS II showing all hydrogeological units within the formations. The abbreviations are explained on Dinoloket.

2.3.3 Research areas

This study mainly focuses on the south-western and central part of the Netherlands, where the research areas, the ZZR and WBR, are located. A cross section of the lithostratigraphy in these regions, made by the models DGMdiep v5.0, BRO DGM v2.2 and BRO REGIS II v2.2.2 are shown in Figure 2-6. In the WBR, the depth of both formations increases to the northeast, where it encounters several faults and in the basin of the RVG. In the ZZR, the lithostratigraphy has a synclinal shape and a deepest point is reached in the ZZL.

The Oosterhout Fm increases in thickness towards the northwest in both the ZZR and WBR. The geohydrological units are mostly constant in thickness and distribution in the research areas. The Breda Sg increases in thickness in the RVG and ZZL. The sandy part of the Breda Sg, however, is the thickest in the southeastern part of both research areas and decreases in thickness toward the northwest, where clay is the more dominant lithology in the Breda Sg.

3 Methodology

3.1 Data analysis

Data on the presence and quantities of glauconite in shallow wells (<500m) was extracted from the Dinoloket database. In the standard borehole description methodology, glauconite content is described when present. For most wells, a glauconite fraction is given, indicating the presence of glauconite (Table 2-1). In more recently drilled wells, glauconite is described in percentages instead of fractions, creating more precise dataset for these wells. This lithological dataset is used to get an impression of the distribution of highly glauconitic lithologies. In the determined research areas and a few other elaborately described wells, the lithological data is compared to the available well logs, with the main focus on the GR, SGR and SP.

The deep wells documented on NLOG were analysed too, as the Breda Sg reaches depth below the 500m. However, the data density of deeper wells is lower and the deep data is mostly documented in pdf and image files with litholgical data, instead of a searchable database, Which made it difficult to filter out glauconite data and create an overview. Moreover, the presence of glauconite is in most cases just noted down as an observation without any quantification method, making it impossible to distinguish between lithologies that contain only a few glauconite grains and glauconite rich sands.

The available data on Dinoloket and NLOG, together with the cutting analysis was used to map with QGIS the wells in which high glauconite intervals were found. The petrophysical and lithological logs were compared and correlations between GR, SGR and SP measurements and glauconite content were analysed. Based on the precision of the glauconite description and the different petrophysical well logs available in the wells, the wells in and around the research areas that were most useful for this research were selected for more elaborate analysis (Table 2-2).

Table 3-1: Glauconite fraction classes and their corresponding description and percentages.

Code of glauconite fraction class	Described amount of glauconite	Glauconite percentage M_L (%)
GC0	Geen glauconiet	$M_L = 0$
GC1	Spoor glauconiet	$0 < M_L \leq 1$
GC2	Weinig glauconiet	$1 < M_L \leq 10$
GC3	Veel glauconiet	$10 < M_L \leq 30$
GC4	Zeer veel glauconiet	$30 < M_L \leq 50$
GC5	Uiterst veel glauconiet	$M_L > 50$
GCX	Onbekende hoeveelheid glauconiet	$0 < M_L \leq 100$

Table 3-2: All wells that were selected for more detailed analysis, depending on their available petrophysical well logs and glauconite data.

Well name	Glauconite description	Petrophysical well logs available
B39F0836 Zetten	Fraction class	GR, SGR, SP, Resistivity
B39H0235 Druten	Fraction class	GR, SP, Resistivity
B40D2829 + B40D2834 Bemmel/Lingewaard	Precise percentage	GR, SGR, Resistivity
B43G1411 Kruisland	Precise percentage	GR, Resistivity
B44C0215 Prinsenbeek	Fraction class	GR, SGR, Resistivity, Density, Neutron
B44E0146 Hank	Fraction class	GR, SGR, SP, Resistivity, Density
B44E1121 Drongelen*	Precise percentage	GR, SGR, Resistivity
B49E1446 Bergen op Zoom	Precise percentage	GR, Resistivity
B49E1470 Kruisland	Precise percentage	GR, Resistivity
Amstelland-01 (AMS-01)	Precise percentage	GR, SGR, Sonic, Resistivity, Density, Neutron, PEF
Hilvarenbeek-01 (HVB-01)	Precise percentage	GR, SGR, SP, Sonic, Resistivity, Density, Neutron, PEF
Jutphaas-01 (JUT-01)	Precise percentage	GR, SP, Sonic, Resistivity
Oranjeoord-01 (ORO-01)	Precise percentage	GR, SGR, Sonic, Resistivity, Density, Neutron, PEF

**The analysis of the Drongelen well B44E1121 is given in Appendix E.*

3.2 Cutting analysis

In the ZZR, the Breda Sg and Oosterhout Fm are too deep to be included in most shallow wells on Dinoloket. The wells that reach this deeper domain are found on NLOG, but without elaborate lithological descriptions or quantitative analyses on glauconite content. To enhance the rather limited dataset in this area, cuttings were analysed from the four deep wells AMS-01, HVB-01, JUT-01 and ORO-01. Of each well, the washed dry cuttings of the interval identified as the Oosterhout Fm and Breda Sg were used (280-600m in AMS-01, 140-520m in HVB-01, 280-840m in JUT-01 and 100-300m in ORO-01). These cuttings were available at the TNO Central Core Sample Storage. The cuttings from the AMS-01 and 100-260m interval of ORO-01 were collected every 20m MD, and the cuttings from HVB-01, JUT-01 and the 260-300m interval of ORO-01 every 10m MD. The cuttings were analysed by firstly observing the overview of the samples and secondly observing the smaller grains with the microscope and identifying different lithological components present. The main lithology, sand median class, mica fraction, glauconite fraction, shell percentage and silt, sand and humus admixture were all estimated and described.

Of each sample, a microscopic image was made as well, which could be used for image processing. Using the Fiji software by ImageJ, a more precise glauconite percentage was calculated. For each specific image, the RGB color range and brightness of the glauconite grains is selected. As a result, the software will select everything in the selected color range, which should correspond to surface of the glauconite grains only. A binary image is created from this selection and used to calculate the total area percentage of the selected surface, corresponding to the glauconite percentage of the sample (Figure 3-1).

To test the methodology and quantitive analysis methods, the image analysis was also done on some samples of the Drongelen wells (B44E1121 & B44E1124) and one sample from the Kruisland well (B49E1470) and one from Antwerpen, used in the research of Piedrabuena . The results of the image analysis were compared with the visually estimated values in the borehole descriptions, as well as the results of the XRD analysis from (2024) and Korevaar (2023).

Moreover, the unwashed cuttings from the 200-300m interval of the ORO-01 well were analysed to compare the unwashed cuttings with the washed cuttings.

In cooperation with Deltares, a few cuttings were also measured by a Portable Gamma Ray Spectrometer GS-512i. Shielded as much as possible from background radiation, this instrument was placed on top of each individual cuttings to measure the SGR signal of a single sample. However, soon it became apparent that the amount of cutting material was too low to be detected by the spectrometer. Therefore it was decided not to continue the measurements after only a few samples were measured.

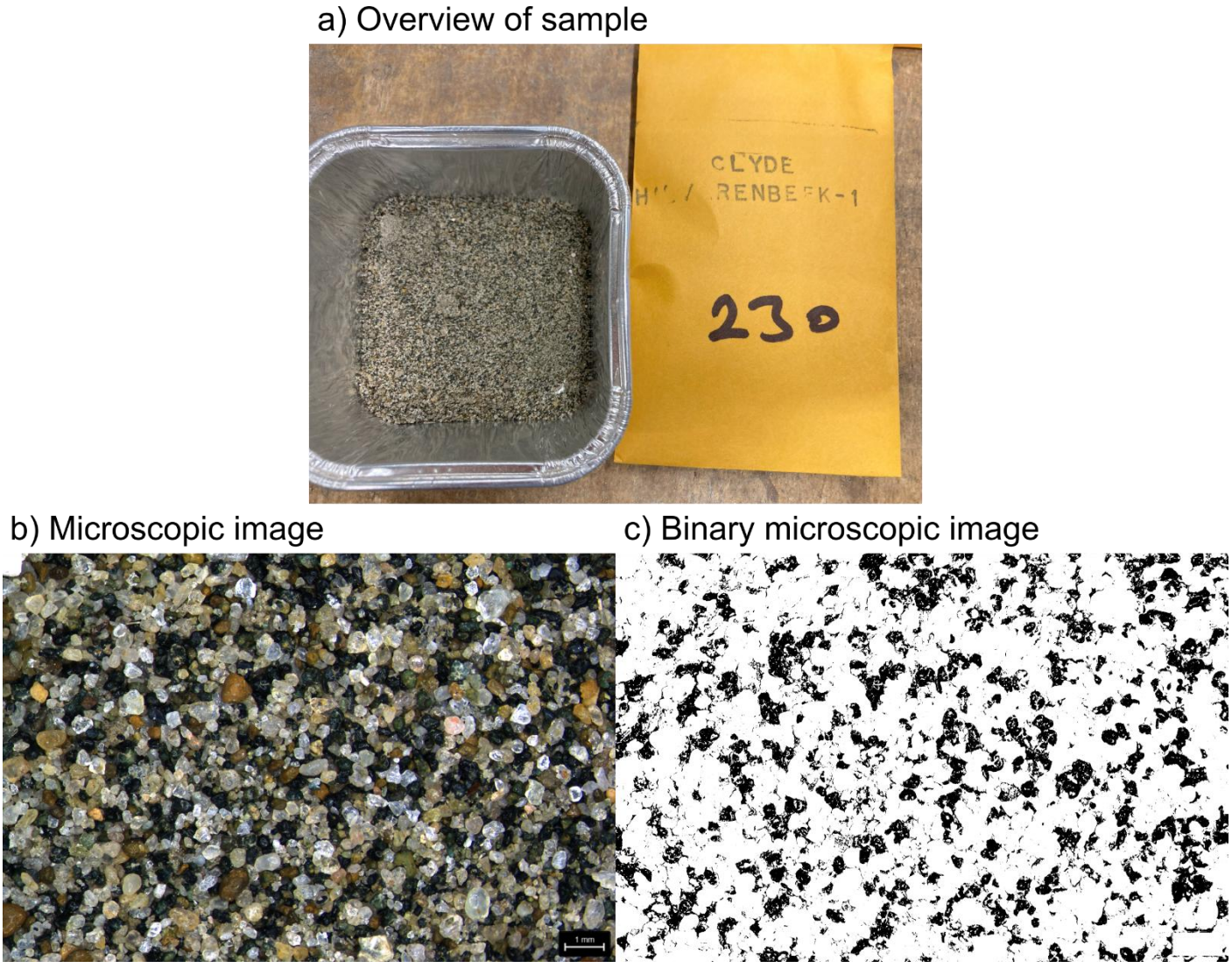

Figure 3-1: a) Sample from HVB-01, 220-230m MD. b) Microscopic image of the sample. c) Binary image with only the glauconite grains selected based on their colour.

3.3 Calculations

To be able to compare the lithology data with the petrophysical logs, the petrophysical log data was used to calculate the Vshale. This Vshale indicates the fraction of shale or clay in the wall rock material and is often calculated with the GR log using two cutoff values: The 'Clean sand'-cutoff (GR_{sand}) and the '100% shale'-cutoff (GR_{shale}). The values of these cutoffs are defined by the GR signal in a lithological interval that is known to be a (quartz) sand or a (close to) 100% shale/clay layer, respectively. The Vshale was then calculated with the equation:

$$Vshale = \frac{GR_{log} - GR_{sand}}{GR_{shale} - GR_{sand}}$$

The GR_{log} in this formula indicates the GR value of the point of interest. The same principle is used when the Vshale is calculated from an individual radioactive element (Th, U or K) from the SGR or from the SP log.

While the cutoff are usually determined for each formation separately, in this research the Vshale is calculated with a single sand- and shale cutoff for the whole well. One of the reasons for this approach is to observe the true mismatches in the Vshale calculations and better compare the differences between the formations. Additionally, a cutoff for each separate formation was often not so easy to determine as a 100% shale or clean sand was not always present in each individual formation. Furthermore, the boundaries of the former Breda Fm were based on lithostratigraphy in the shallow wells, while the new Breda Sg and Diessen and Groote Heide Fm are based on lithostratigraphy, complicating the formation-specific interpretation. However, the cutoffs used for the calculation are in some cases redetermined for each formation separately if there seems to be a significant difference between the GR_{sand} or GR_{shale} of the different formations that could be solved by a formation-separate Vshale interpretation.

Furthermore, the effect of different minerals on the SGR and GR was tested. The 'theoretical' GR effect of each mineral was calculated using the values from Table 2-1 and Table 2-2. The contribution of a mineral to the radioactive element content could be calculated with the equation: $X_L = X_M \cdot M_L$. In this equations, the contribution of mineral M to the content of element X in Lithology L (X_L) is calculated with the fraction of the mineral in the lithology (M_L) and the content of X in the mineral (X_M). The effect of the mineral M on the GR log (GR_M) can be calculated with the GR response of element X (GR_X) and X_L: $GR_M = GR_X \cdot X_L$. This theoretical GR-effect of an accessory mineral was useful to unravel the origin of a GR signal and to calculate a new Vshale using the GR signal that was corrected for the GR contribution of glauconite.

4 Results

4.1 Lithology

4.1.1 Distribution of glauconite

In the database of Dinoloket, glauconite content was described in 6689 wells. For most wells, this was done by assigning a class of glauconite fraction to each lithology interval with glauconite mentioned in the description. The glauconite fraction classes and their corresponding percentages and descriptions are listed in table 2-1.

Glauconite was described in many marine deposits in the Dutch subsurface, but large quantities (>10%) commonly occur in the Oosterhout Fm and Breda Sg of the Upper North Sea Group and the Vaals Fm of the Chalk Group. Figure 4-1 shows all the shallow wells in the Netherlands where glauconite is described, as well as the maximum glauconite content that was found in each well. As can be seen in Figure 4-1b and 4-1c, the wells with the highest glauconite content correspond to the wells with high glauconite fraction classes in the Oosterhout Fm or the Breda Sg, except for some wells in Limburg that penetrate the glauconite-rich Vaals Fm.

It is also observed that the wells in the border regions of the Netherlands, in a belt from Zeeland to Groningen, have a higher maximum glauconite content than the wells in the northwestern part of the country. It can also be seen that much more wells penetrate Oosterhout Fm and former Breda Fm in the border region. This border region is also the part of the Netherlands where the Oosterhout Fm and former Breda Fm are located shallow in the subsurface and where they are less thick, meaning that during deposition, the average sedimentation rate was lower as well.

In the database of NLOG, the quantitative information on glauconite content was very limited. Most data on glauconite content was only qualitative (the presence of the mineral was described, but not the amount). Most of the time, this data was only available in graphic composite logs or pdfs of scanned borehole reports, which made it hard and too time-consuming to filter out the limited useful data from NLOG. Therefore, the dataset was extended with the analysed cuttings from deep wells AMS-01, HVB-01, JUT-01 and ORO-01. The results of the cutting analysis are included in Appendix D.

In Figure 4-2, the more elaborately studied shallow wells in and around the research areas, as well as the analysed deep wells, are shown. The colour of the wells indicates the maximum glauconite content encountered in the wells and the separate formations of interest. The lithological and petrophysical logs of a selection of wells are shown in Figures 4-3, 4-4, 4-5 and 4-6.

In the Oosterhout Fm and Breda Sg of the analysed wells, the glauconite content ranges from 0% up to 90%, but the most wells penetrating the formations of interest have a maximum Glauconite percentage of 20-40%. Glauconite percentages higher than 10% are most of the time found in (glauconitic) sand lithologies. Clay and loam lithologies (clay defined as >8% lutum and loam as <50% sand and <8% lutum) can also contain glauconite, often described for the sand fraction of the sediment. These lithologies typically have low amounts of glauconite ranging from 0 to 10%.

While almost all sediments in the Oosterhout Fm and Breda Sg contain some glauconite, the amount of glauconite varies laterally between wells, as well as vertically within each well. Peaks in glauconite content, where significantly more glauconite is found compared to the adjacent lithologies, are identified in the Oosterhout, Diessen and Groote Heide Fm.

In the Oosterhout Fm, a peak is found in the lower part of the formation just below the shell layers of the Sprundel Mb and above the less glauconitic Goirle Mb. In the newest lithostratigraphy this (highly) glauconitic sand is called the Tilburg Mb, and it is recognised in some recently drilled wells, especially in the central part of the province Noord-Brabant. The glauconite peak in the Tilburg Mb is for instance observed in the Goirle well at ca. 100m MD (ca. -80m w.r.t. NAP) (Figure 4-4c).

In the Breda Subgroup, peaks in glauconite content are identified as well. The internal lithostratigraphy is less well-defined and the depth of the MMU, the boundary between the Diessen and Groote Heide Fm, is not yet defined in most wells. Therefore it is hard to define the vertical location of the peaks in glauconite content. In the westernmost part of the WBR, one peak is found in the upper part and one in the lower part of the Breda Sg. In the Kruisland (2) and Bergen op Zoom wells (Figure 4-3b and 4-3c), both peaks can be identified, while only one peak is present in the Kruisland (1) well (Figure 4-3a), where the defined Breda Fm is thinner. In the eastern part of the WBR, the peaks were less significant and instead an trend of constant to upward decreasing glauconite content was observed in the Breda Sg. In the ZZ area, the peaks are also less clear, but glauconite contents of higher than 10% are found mainly in the upper half of the Diessen Fm and in a small part at the bottom of the Groote Heide.

Apart from the glauconite grains, several other accessory minerals and materials were observed in the sediments of the Oosterhout Fm and Breda Sg. Next to the common quartz sand grains, shell fragments and clay minerals, the sediments included organic material (including plant remnants), goethite, phosphate concretions and micas (mainly muscovite). The occurrence of these accessory materials is often semi-quantitatively indicated with a classification system that recognises three different classes in the lithological description of the shallow wells.

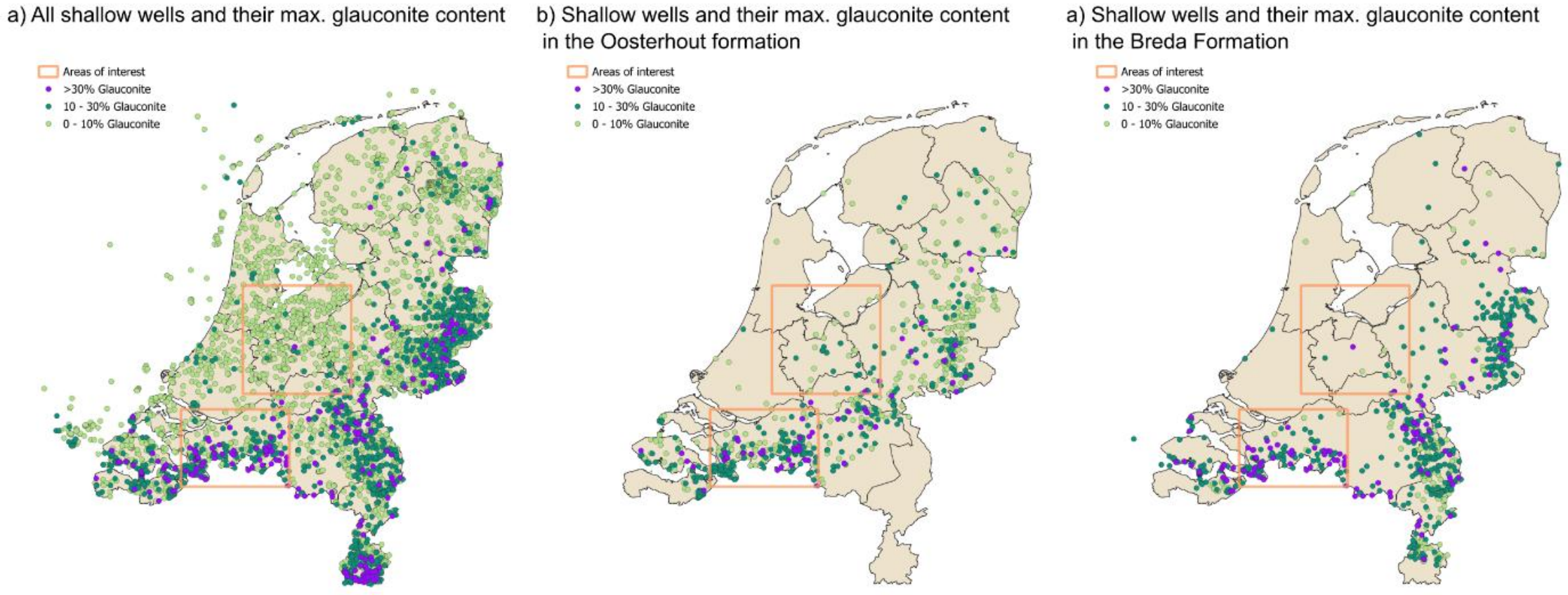

Figure 4-1: a) All shallow wells in the Netherlands where glauconite is described, coloured by the maximum glauconite content. b) Wells where glauconite is found in the Oosterhout Fm, coloured by the maximum glauconite content in this formation. c) Wells where glauconite is found in the Breda Sg, coloured by the maximum glauconite content in this subgroup.

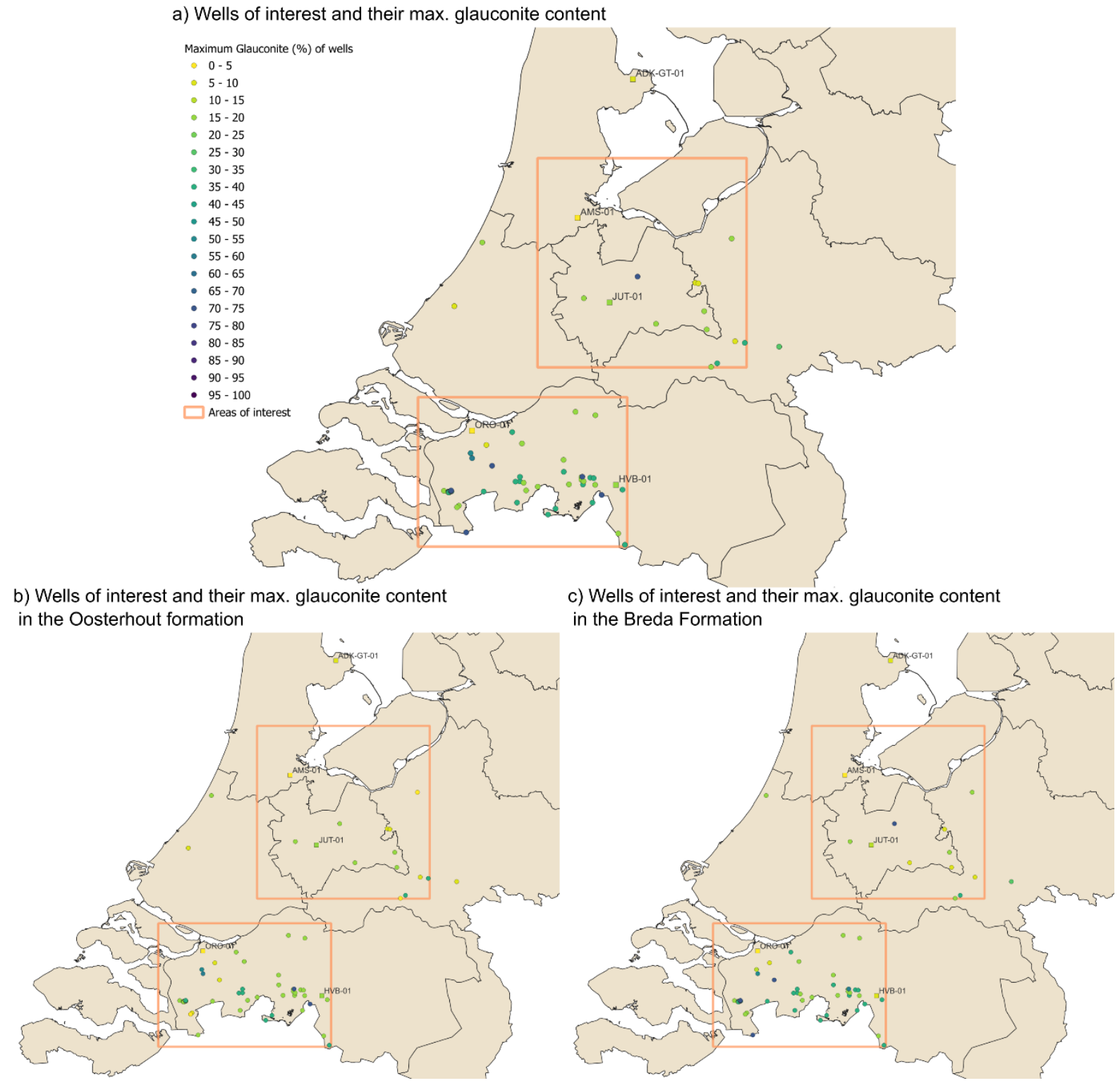

Figure 4-2: a) Wells of interest where glauconite is described, coloured by the maximum glauconite content. b) Wells of interest where glauconite is found in the Oosterhout Fm, coloured by the maximum glauconite content in this formation. c) Wells where glauconite is found in the Breda Sg, coloured by the maximum glauconite content in this subgroup.

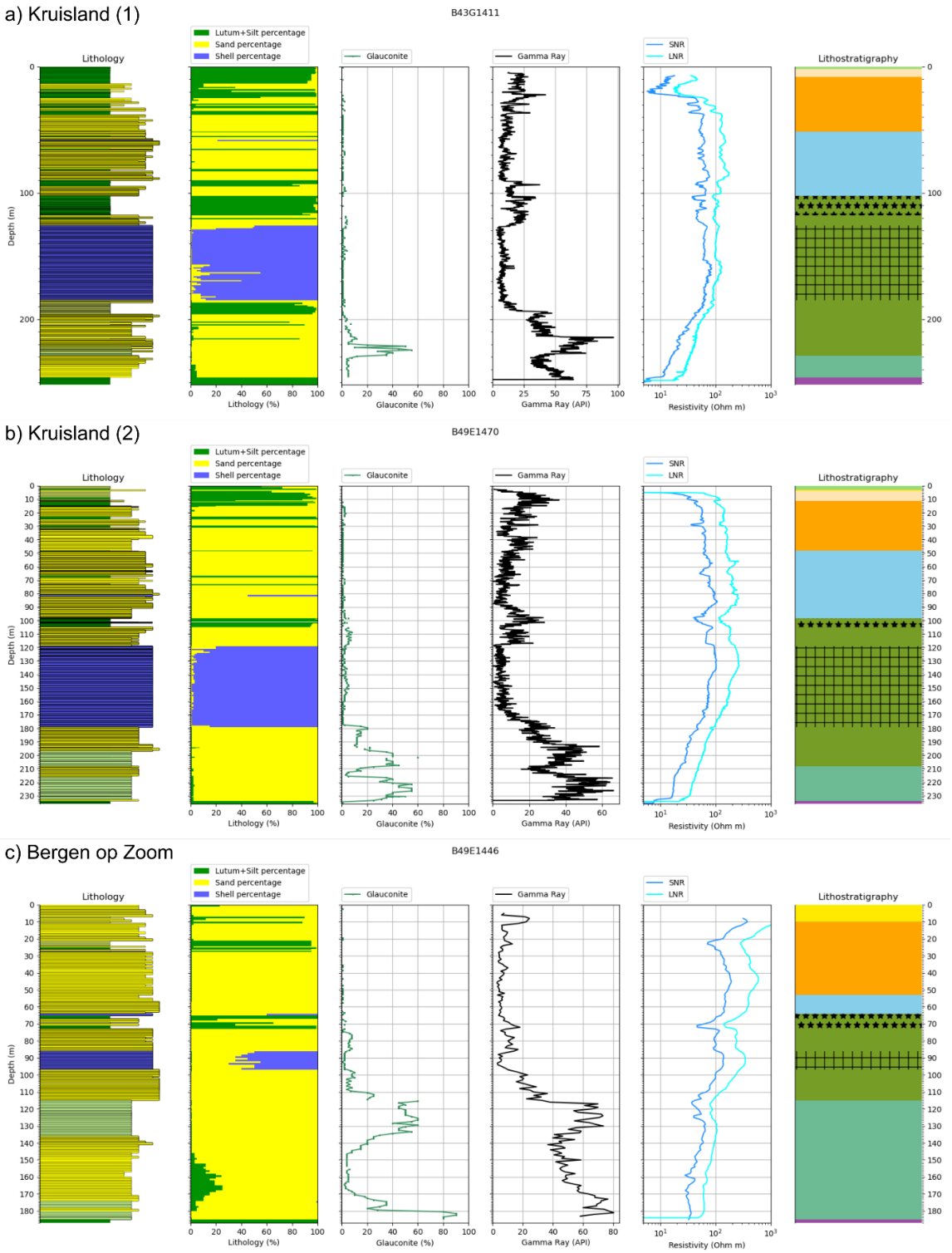

Figure 4-3: Lithology, glauconite content, GR, short normal resistivity (SNR) and long normal resistivity (LNR), and lithostratigraphy of three shallow wells from the western part of the WBR. A legend for the Lithology and Lithostratigraphy columns can be found in Appendix B.

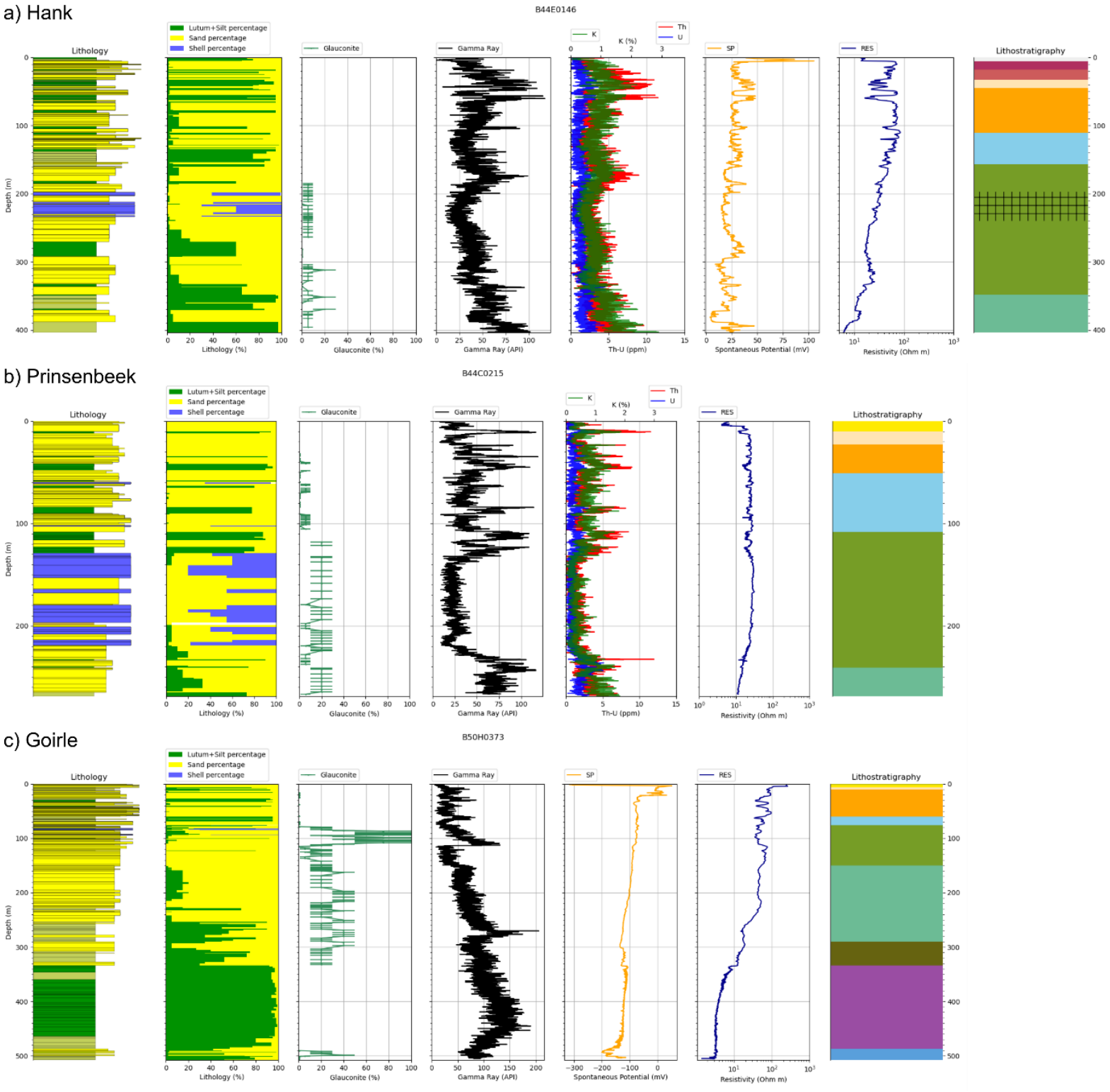

Figure 4-4: Lithology, glauconite content, GR, SGR, SP, resistivity (RES) and lithostratigraphy of three shallow wells from the central and eastern part of the WBR. A legend for the Lithology and Lithostratigraphy columns can be found in Appendix B

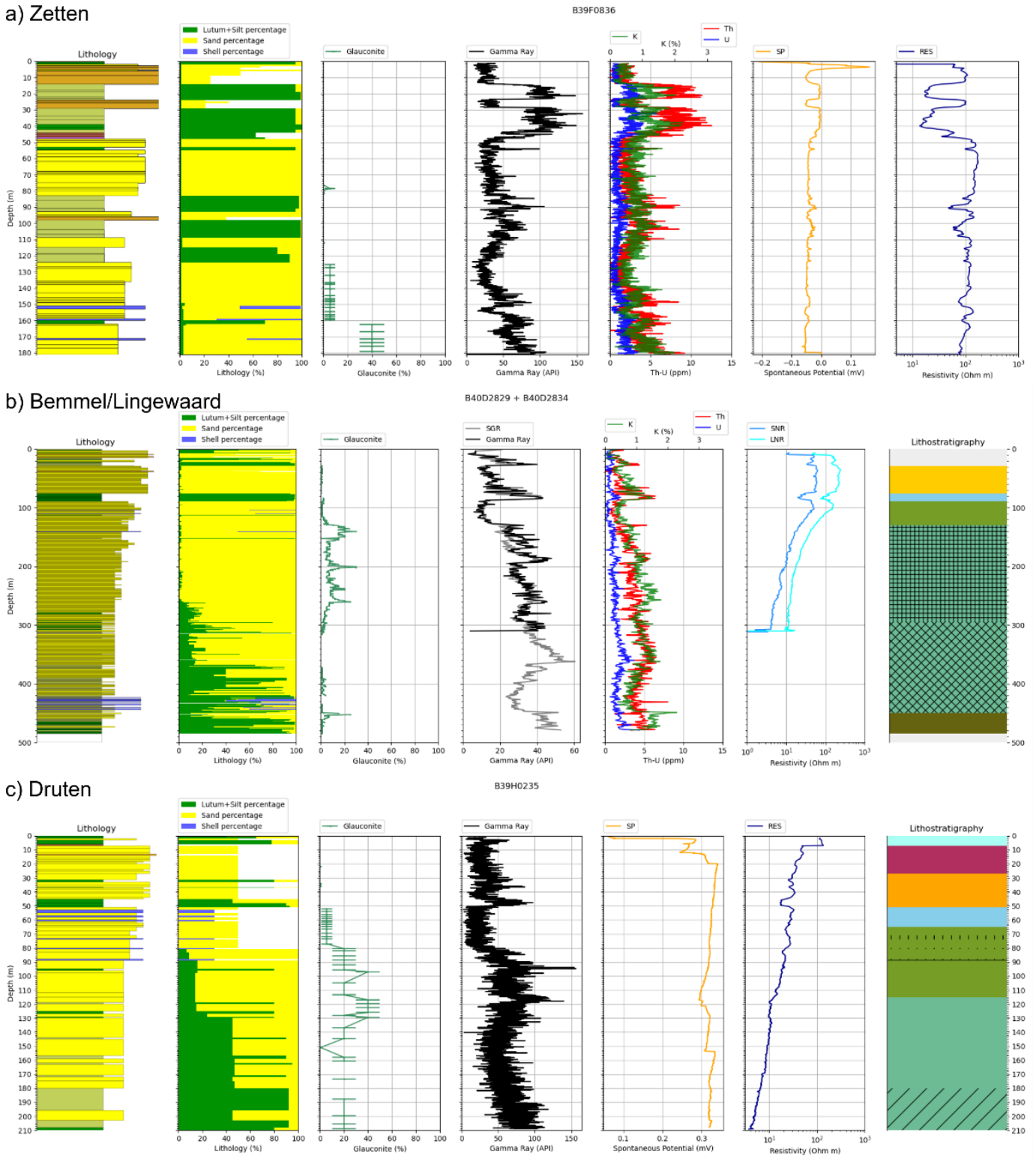

Figure 4-5: Lithology, glauconite content, GR, SGR, SP, resistivity (RES), short normal resistivity (SNR) and long normal resistivity (LNR), and lithostratigraphy of three shallow wells from the southeastern part of the ZZR. A legend for the Lithology and Lithostratigraphy columns can be found in Appendix B.

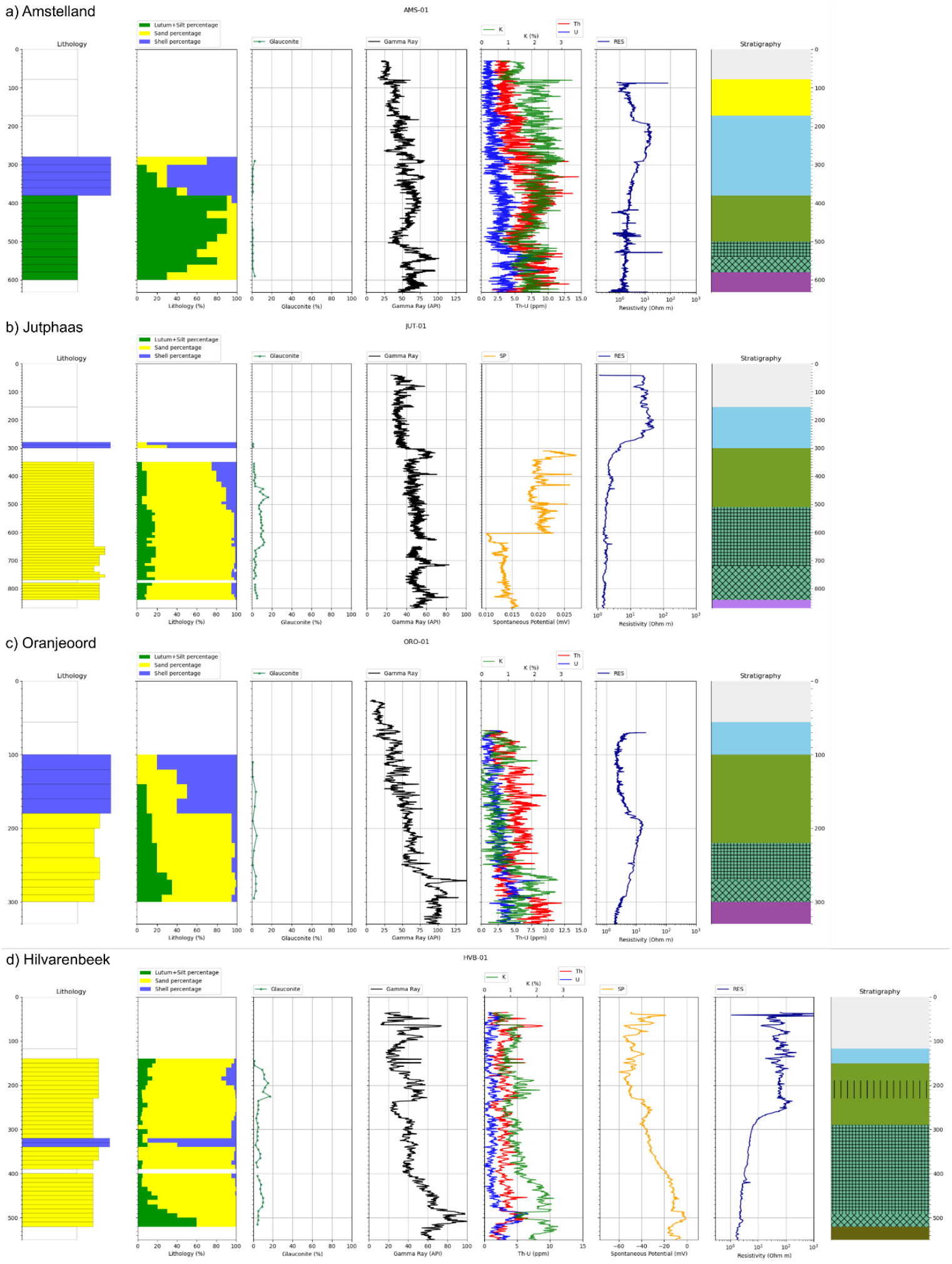

4-6: Lithology, glauconite content, GR, SGR, SP, resistivity (RES), and lithostratigraphy of the four analysed deep wells from the ZZR and WBR. A legend for the Lithology and Lithostratigraphy columns can be found in Appendix B

4.1.2 Appearance of glauconite

The appearance of the glauconite grains in the cutting samples was studied as well as their quantity. Overall, the colour ranges from light green to darker green to bluish black, the size ranges from silt size to medium fine sand and the shape is mostly rounded, where some grains have a smooth surface and other are more bulgy grape cluster shape. A number of examples are shown in Figure 4-7. Based these variations in appearance, three types of the most commonly found glauconite grains were defined:

1. Light green and small pellets
   This type of glauconite grain is typically (light) green in colour and has a size that ranges from 10 µm (silt) to 200 µm (fine sand). The shape of the grains is mostly round or oval and sometimes angular as well (Figure 4-7a). Some of the larger light green grains can have a somewhat more bulky surface (Figure 4-7d). This type of glauconite was never found in high amounts of more than 5% and in sands it often coexists with glauconite grains of categories 2 and 3. In glauconitic loam and clay lithologies, this type of glauconite is the most common.
2. Bulky grape clusters
   This type of glauconite grain is more commonly found in the Breda Sg and Oosterhout Fm than the first type. It is darker in colour than the first type, ranging from (dark) green to bluish black. The bluish black grains are more commonly found, but the inner material of the grain always shows a green colour when it is crushed. This type occurs in a large range of sizes, from 80 µm (very fine sand) up to 1 mm (very coarse sand). Its shape is very characteristic, as it is mostly bulky and often reminds one of a grape cluster (Figure 4-7c). This type often coexists with both other types and can be present in larger quantities.
3. Dark smooth pellets
   The oval pellet-like shape and smooth surface are the main characteristic for this type. Similar to type 2, the colour ranges from (dark) green to bluish black, but when crushed, the colour of the inner part of the grain is always green (Figure 4-7e). The grain size ranges from 80 µm (very fine sand) to 500 µm (coarse sand). It is mostly found in sandy lithologies and while it is often found together with other types of glauconite, it can be dominating in a sediment sample, as can be seen in Figure 4-7b.

It was difficult to distinguish any clay-size glauconite (< 2 µm) with the microscopic method. However, it was observed that some loamy and clayey samples had a greenish colour that was not directly linked to large glauconite grains, which could be an indication of some glauconite material mixed in the clay fraction.

The different types of glauconite occur in different amounts over depth as well. For the glauconite peaks mentioned before, the glauconite peak in the Tilburg Mb is mainly dominated by glauconite grains of darker type 1, with some grains of the other two types (Figure 4-7d). In the upper part of the Breda Sg the type 1 glauconite is relatively more abundant in the sands as well, but still the type 2 glauconite is most abundant. In the lower part of the Breda Sg, the type 3 glauconite is more dominant (Figure 4-7b).

The three different types of glauconite could be linked to the different stages of glauconite evolution. Type 1, the light green and small pellets, were interpreted as Nascent to slightly evolved glauconite. Type 2, the bulky grape clusters, were interpreted as evolved glauconite and type 3, the Dark smooth pellets, as highly evolved.

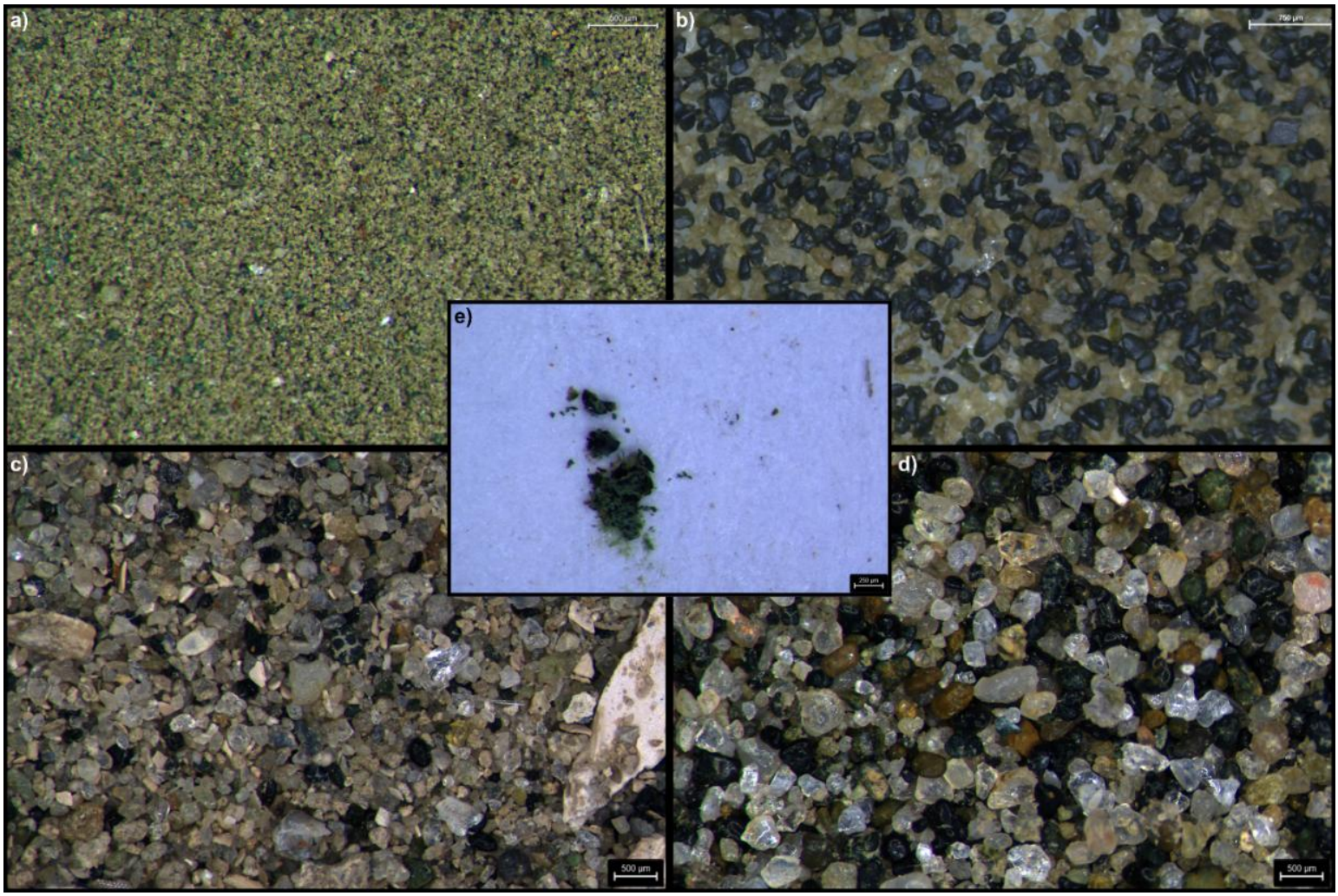

Figure 4-7: Different modes of appearance of glauconite found in the Dutch subsurface. a) Silt fraction sample from the Drongelen well B44E112,1 421-422m MD, with silt-sized light green small pellets of type 1,. b) Glauconitic sand sample from Kruisland (2) well B49E1470, 230.4-230.7m MD, with dark smooth glauconite pellets from type 3. Image derived from Korevaar ***(2023)****. c) Cutting from JUT-01, 450-460m MD, with a Bulky grape cluster glauconite of type 2 in the middle of the image. d) Cutting from HVB-01, 220-230m MD, with glauconite grains of all three types together. e) Crushed glauconite grain from HVB-01, 230-240m MD. While the outside is dark bluish black (type 3), the inside of the grain is green.*

4.2 Petrophysics

In many wells, the GR and resistivity was measured and in some wells, additional logs such as SP, SGR and/or other well logs were available (Table 2-2). The analysed deep wells had a larger array of available well logs than most shallow wells.

4.2.1 Spectral Gamma Ray

In the wells where a SGR log was measured in (a part of) the borehole, the lithology data was compared to the SGR measurements. In Figures 4-3, 4-4, 4-5 and 4-6, the lithological, GR and SGR logs are shown.

A Th-K mineral map, introduced in Section 2.2.1 and Figure 2-2b, was also made for each well with SGR data (Figure 4-8). In the wells HVB-01 and Bemmel/Lingewaard (B40D2829+B40D2834), it is observed that higher glauconite content plots closer to the glauconite field in the Th-K mineral map. This is not observed in the less glauconitic AMS-01 and ORO-01 wells, and the other two shallow wells, where glauconite is described in fraction classes instead of percentages.

For the wells with precise glauconite percentages described and a SGR available, the Th/K ratio was also plotted against the glauconite content (Figure 4-9). This was done on a linear and a log-log plot, with the data coloured by depth. Again in the wells HVB-01 and Bemmel/Lingewaard (B40D2829+B40D2834), it is observed that higher glauconite content has a lower Th/K ratio. In ORO-01, the data is quite scattered and some really high Th/K ratios are measured. In AMS-01, no trend is visible as data of high glauconite contents is missing, but the data of low glauconite contents fits with the overall trend of HVB-01.

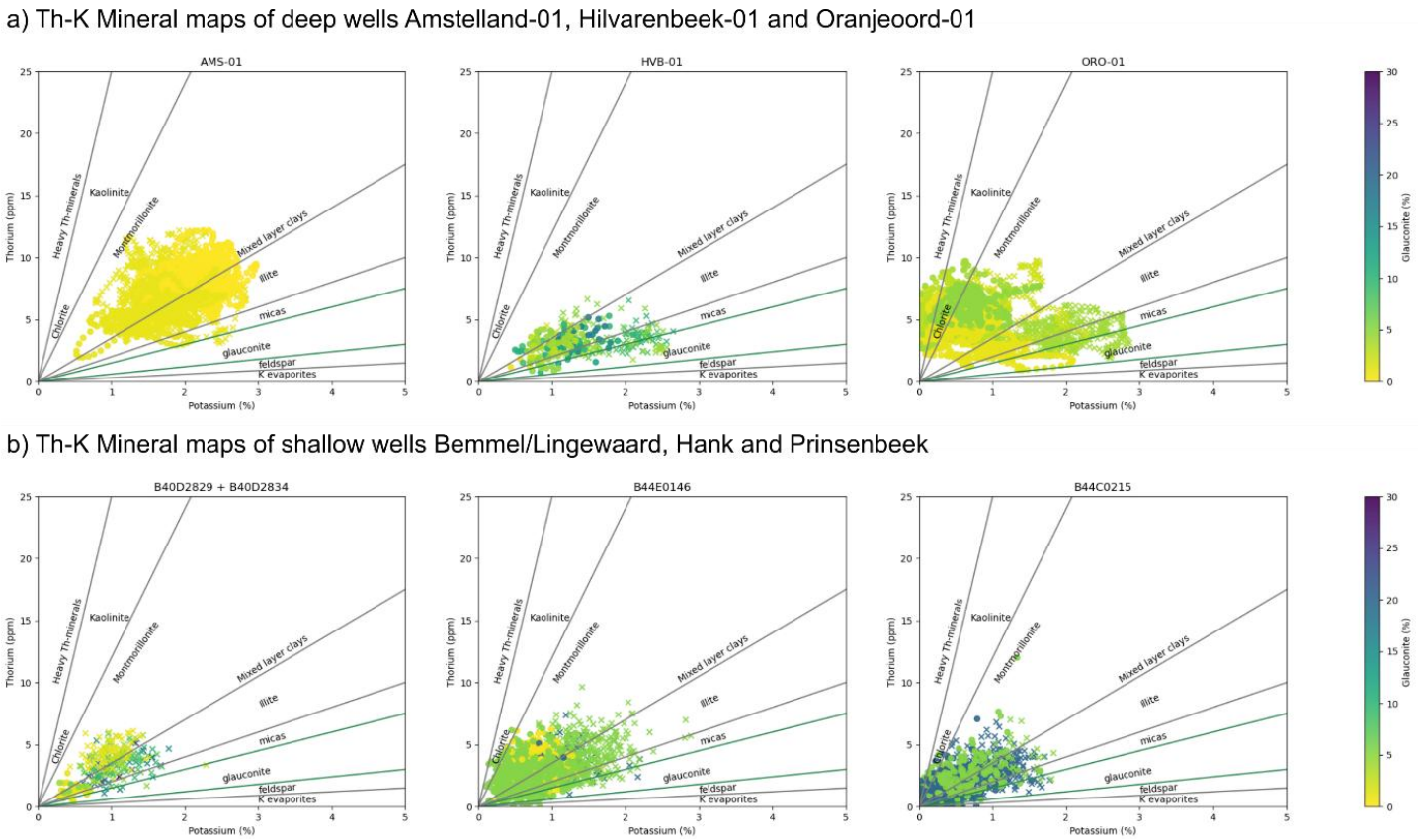

Figure 4-8: Th-K mineral maps of the deep wells from Amstelland, Hilvarenbeek and Oranjeoord (a) and the shallow wells from Bemmel/Lingewaard, Hank and Prinsenbeek (b). The datapoints are plotted according to the Th and K content measured by SGR and coloured by the described glauconite content of the lithological interval with corresponding depth.

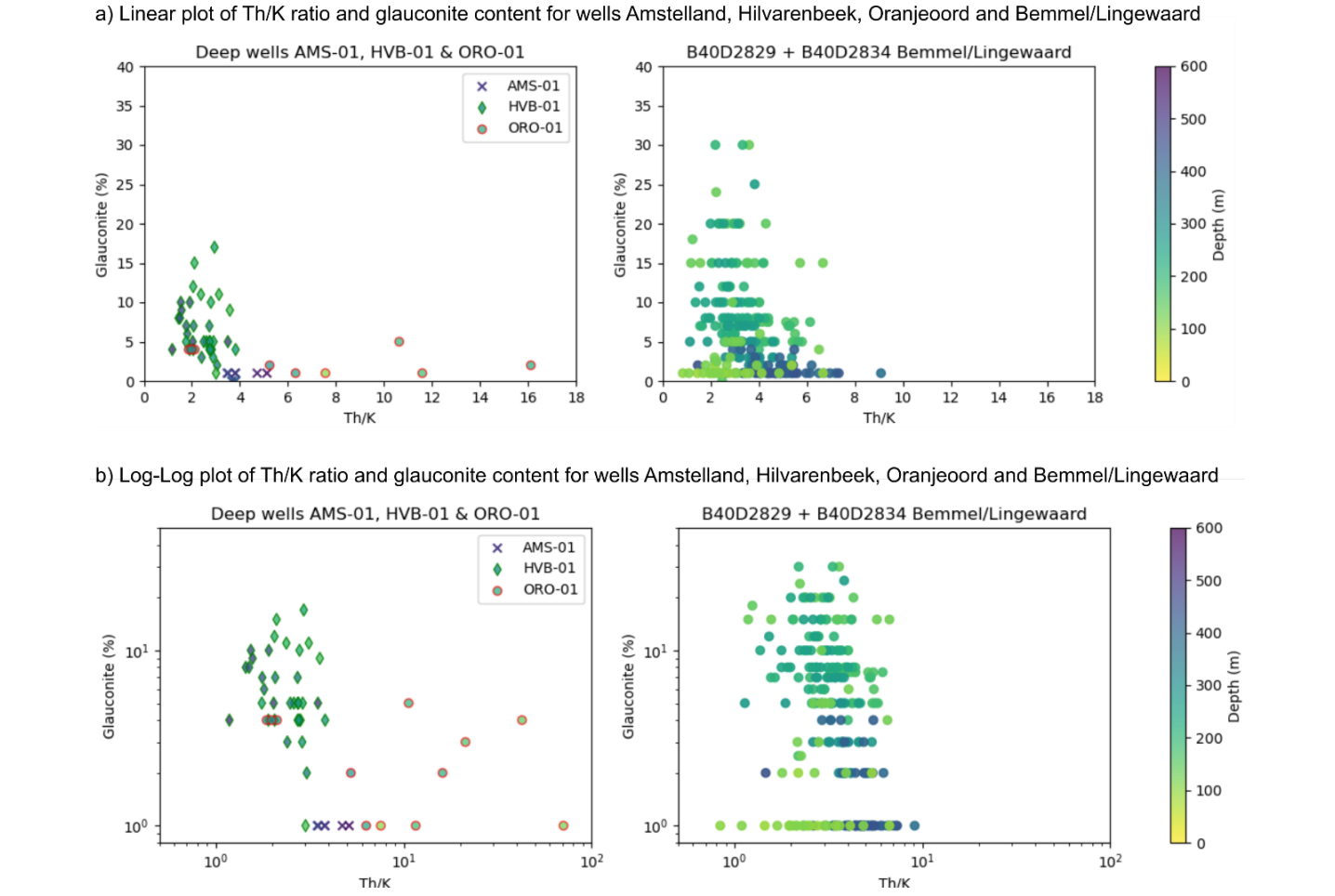

Figure 4-9: Glauconite percentage and average Th/K ratio per lithological interval on a linear (a) and Log-Log (b) plot. The dots are coloured by the depth of the lithological interval.

4.2.2 Vshale calculations

For several wells, the Vshale was calculated from the petrophysical logs. The Vshale results from different logs, as well as the GR with glauconite correction (with the theoretical contribution of glauconite subtracted, as described in Section 3.3), are shown in Figure 4-10 and 4-11. The results are described for each type of Vshale log below.

1. Vshale from GR (not corrected)

   For the formations younger than the Oosterhout Fm, the Vshale from the GR is often in line with the observed Lutum + Silt percentage observed in the well. Examples where the Vshale reflects the alteration of sand and clay layers can be seen in Bemmel/Lingewaard B40D2829+B40D2834 70-100m MD, Kruisland (1) B43G1411 70-120m MD and Kruisland (2) B49E1470 10-50m MD. In the lower Oosterhout Fm and the Breda Sg, the Vshale from GR overestimates the shale volume if no corrections are applied.

   In some cases a Vshale is given from the GR (cutoff per Fm), which does not have 1 cutoff for the whole well, but has a separate cutoff for each individual formation, as is usually done in petrophysical analysis. In some cases, such as the JUT-01 well, the result do not change a lot if the cutoff is chosen per formation. For most wells, however, the Vshale log does change and shows a better match, especially in the Breda Sg. On the other hand, there are often peaks in this Vshale that indicate a 80-100% shale, where 0-10% clay is observed, such as in Kruisland (2) B49E1470 220-230m MD, HVB-01 190-240m MD and 480-490m MD and JUT-01 710-720m MD.

2. Vshale from GR (GC correction)

   The Vshale with glauconite correction (GC correction) is corrected for the theoretical GR response that is expected from the observed glauconite. This results in a better match where the glauconite content is substantial, such as in Bergen op Zoom B49E1446 110-135m MD, Kruisland (1) B43G1411 220-230m MD, Kruisland (2) B49E1470 200-210m MD and 220-230m MD and HVB-01 190-240m MD. Other intervals, where not much glauconite was observed, do still have >80% Vshale result, while an almost 100% sand is observed, such as Bergen op Zoom B49E1446 140-180m MD, Kruisland (1) B43G1411 200-220m MD, Kruisland (2) B49E1470 190-195m MD and 210-215m MD and HVB-01 430-460m MD.

3. Vshale from SGR (U, Th and K) log

   The Vshale from U is not shown in the Figures, as the peaks did often not reflect many shale lithologies, but rather peaks occurring near the Miocene unconformities (EMU, MMU and LMU).

   The Vshale from K does not differ much from the Vshale of the total GR. This Vshale indicates a shale in glauconitic sands, like in Bemmel/Lingewaard B40D2829+B40D2834 180-380m MD and HVB-01 190-230m MD and 280-480m MD. In the well ORO-01 260-290m MD, a large overestimation of the shale volume is also observed in an interval with a low glauconite content. The highest peaks in the Vshale that overestimate the shale volume in Breda Sg are however less high, for instance in Bemmel/Lingewaard B40D2829+B40D2834 340-360m MD, AMS-01 500-540m MD and HVB-01 490-500m MD.

   The Vshale from Th is more similar to the described lithologies, but still contains a number of cases where the Vshale indicates a more shaly lithology than the lithological description. A good match between the Vshale of Th and the lithology is observed in HVB-01 and ORO-01, for instance. In in Bemmel/Lingewaard B40D2829+B40D2834, especially at the 130-300m MD interval, the Vshale of Th also shows some Shale peaks in sandy lithologies.

4. Vshale from SP or resitivity log

The Vshale of SP also matches better with the observed lithology. The pattern is similar to that of the Vshale of Th in HVB-01. In the well JUT-01 the Vshale from SP and GR are mostly similar, but some Shale peaks in GR, that are not observed in the lithology, are not visible on the Vshale of SP, such as at 710-720m MD. There are however also sand and shale peaks in the Vshale of SP that differ from the observed lithology, such as in 600-610m MD, 680-690m MD and 820-840m MD in JUT-01.

5. Vshale from other petrophysical logs

The Vshale from Neutron and Density log (ND), only visible in well ORO-01, shows a similar pattern to the Vshale from GR mostly. The shale peak at 270m MD, for instance, is visible in the Vshale of GR and ND, but not in the Vshale of Th and the lithological observation.

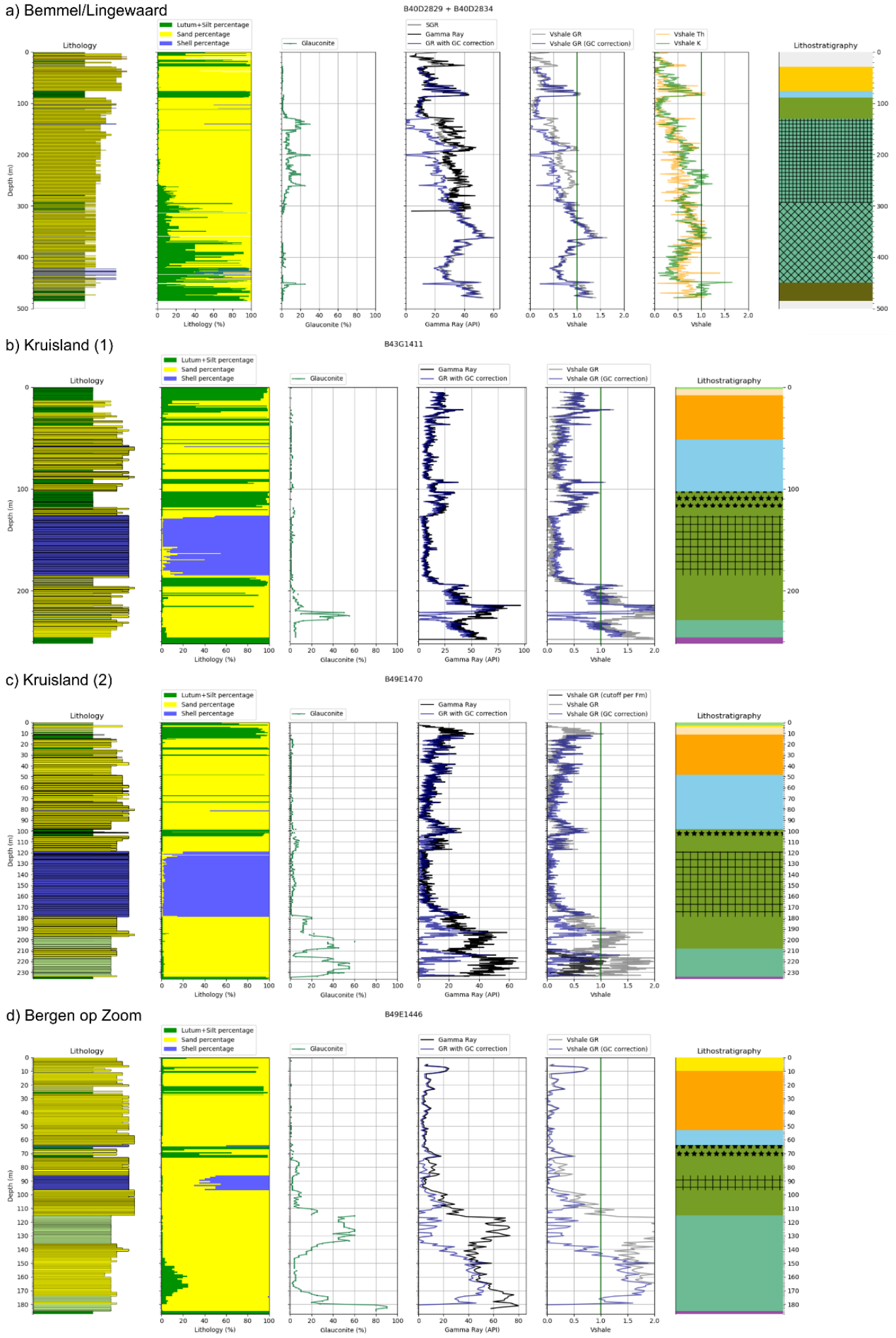

Figure 4-10: Lithology, glauconite content and lithostratigraphy, together with the GR, the glauconite-corrected GR and the results of the Vshale calculations of four shallow wells.

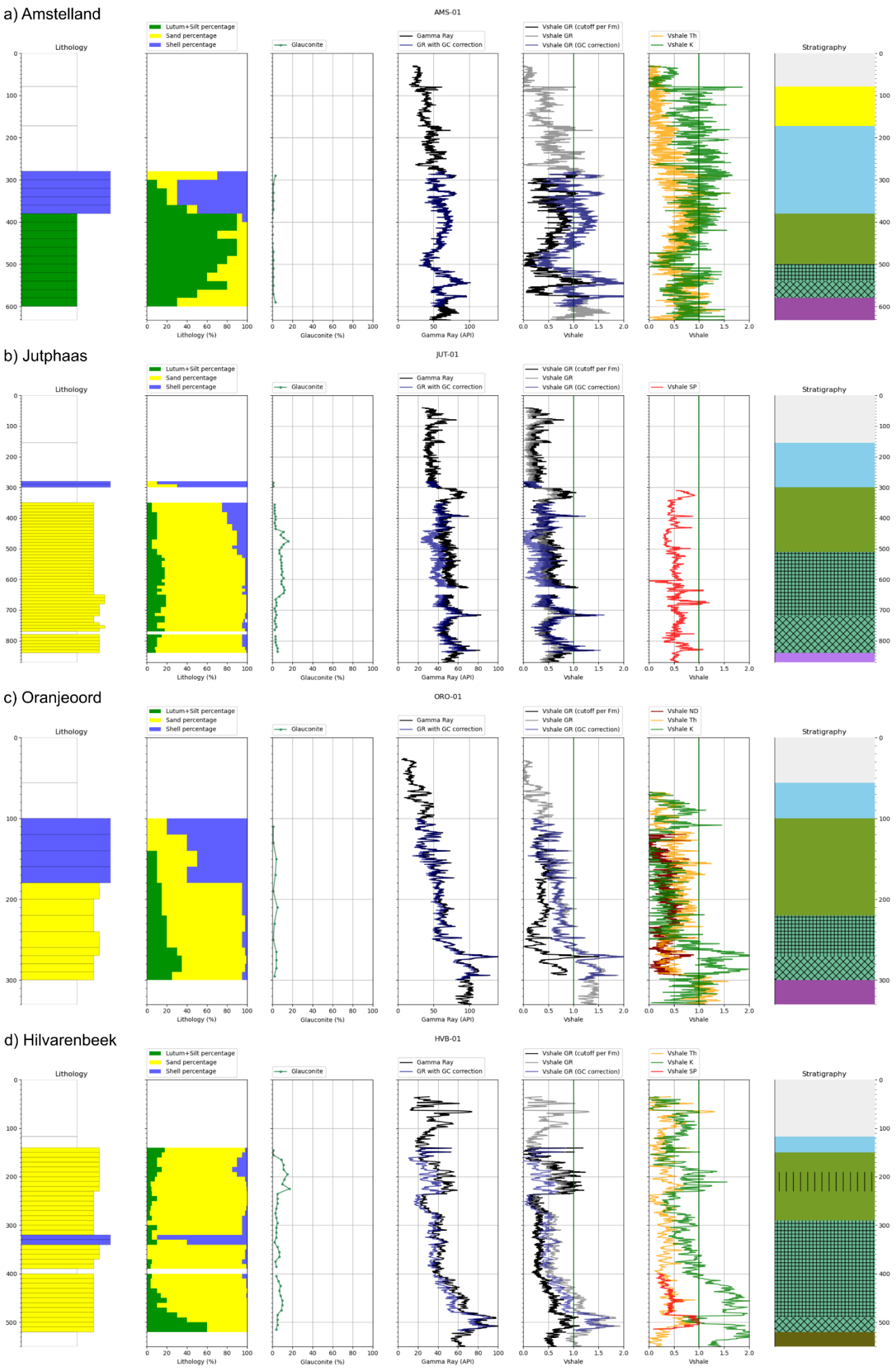

Figure 4-11: Lithology, glauconite content and lithostratigraphy, together with the GR, the glauconite-corrected GR and the results of the Vshale calculations of the four analysed deep wells from the ZZR and WBR.

5 Interpretation & discussion

5.1 Validity and limitations of research methods

5.1.1 Limitations of the datasets

The data on glauconite content derived from Dinoloket and NLOG was provided in different ways. The older shallow wells, with the glauconite content described by the classification of Table 2-1, are officially defined as ranges of percentages (Bosch 2000). These ranges of percentages are too large to do some useful analyses. Furthermore, the glauconite fraction class was often based on a written description that rather tells something about the relative amount of glauconite within one well. It cannot be assumed that the same description automatically infers the same glauconite percentage between different wells. In most deep wells from NLOG and a number of shallow wells, no quantification was given at all and their well description could only be used to identify the presence of glauconite.

In the well JUT-01, a few descriptions of the glauconite content were available. The sediments were described as 'slightly glauconitic' at ca. 430m MD, as 'highly glauconitic at ca. 500m MD and as 'less glauconitic' at ca. 780m MD. Apart from the low resolution of these descriptions (which were the only three sediment description in the interval of interest that was 500m thick, the description were also rather relative. Based on the standard cutting description methods, as shown in Table 3.1, a difference in glauconite percentage of at least 20% was expected between the 'slightly glauconitic' and 'highly glauconitic' sediments. Instead the cutting analysis showed that the glauconite content ranges between 3% glauconite ('slightly glauconitic') and 15% ('highly glauconitic'), which is a much smaller difference than expected. Other glauconite fractions, often derived from written descriptions, can also be a more relative description, showing relative glauconite content differences within one well rather than assigning a specific glauconite content to a sediment.

In the more recently described wells, more precise glauconite percentages are provided. This quantification method has two advantages. First, it is a more precise way to indicate the glauconite content than the range indicated by a glauconite fraction class. Second, the percentage is directly derived from the sample, using the diagrams of Appendix C, instead of being derived from a written relative description. Nevertheless, this quantification method also has its limitations. The percentages are based on a visual estimate and have a certain human error. This error is mainly created when the sample is compared to the visual estimate diagram. For higher percentages, the error of the visual estimate increases, as the diagram charts become harder to distinguish. The human error also depends on the judgement of what counts as a representative part of the cutting to use for determining the estimated percentages.

5.1.2 Limitations of the cutting analysis

When the cuttings from the deep wells were analysed, a similar method was used to provide a glauconite percentage. In this case, however, an area percentage was calculated with image analysis, in addition to the visual estimate. This reduced the human error that is created when the samples are compared to the diagrams of Appendix C. The human error resulting from choosing a representative sample still remains. Additionally, as the image analysis is based on the colour difference between glauconite grains and the rest of the sample, the accuracy of the calculated percentage decreases when other materials with a partly overlapping colour range were present, such as organic charcoal and peat.

When the glauconite content from the image analysis was compared to the visual estimates of Dinoloket and XRD measurements that were done on a number of samples, the average uncertainty of the determined glauconite content was ca. 0.2 x the total glauconite content. Thus, a glauconite content of 10% had an uncertainty of $\pm 2\%$, while a glauconite content of 25% had an uncertainty of $\pm 5\%$.

Other limitations originate from the drilling, sampling and preservation of the samples. Most glauconite content estimates in shallow wells were derived from sediment cuttings representing a 1 m interval, but the cuttings of the analysed deep wells, which were small bags of sediment that was sometimes barely enough to fill a petri dish, often represented a 10 m or even 20 m interval. How representative the cuttings are for the walls rock is hard to tell, but one can imagine that a lot of material is lost in the drilling process and a cutting is never completely similar to the wall rock material. The cuttings are cut loose by the drill bit and carried to the surface with the circulating drilling fluid. This results in a certain amount of mixing of the cuttings, depending on the drilling technique (Veldkamp et al. 2022).

Moreover, the glauconite grains, which are weaker and break down more easily than quartz sand, can be relatively underrepresented in the cuttings when it is destructed in the drilling process. Small scale variations will be lost and the sediment of different horizontal surfaces will be mixed together during the sampling. The original wet cuttings were also washed, dried and kept in storage, before they became the dry washed cuttings used for the analysis. During the washing, the drilling mud, as well as most of the fine silt and clay-sized sediments are removed to increase the visibility of the different sand-sized grains in the sample.

The effect of the washing process was investigated by comparing washed and unwashed cuttings. It was more difficult to select the glauconite grains by colour for the unwashed cuttings, as the dark silt and mud showed less contrast with the glauconite grains as the sand fraction. The difference between the glauconite percentage from washed and unwashed samples was not more than 4%, and often only 1 or 2%, similar to the determined uncertainty range. As the glauconite identified in the unwashed cuttings had similar grain sizes in the washed cuttings, the washing process probably did not have a large effect on the glauconite content of the sample.

5.1.3 Limitations of the petrophysical well logs

The petrophysical well logs also have their limitations. The GR and SGR log for instance, do not only measure radiation from clay layers and accessory minerals, but can also detect cosmic background radiation and gamma radiation from barite and KCl in the drilling mud. Furthermore, the GR signal of the sediments has to travel through the wall rock and the borehole, and it loses part of its energy on its way. Therefore the density of the drilling fluid and the wallrock, as well as the logging speed and the borehole diameter all effect the intensity of the GR signal. The SGR also automatically interprets the gamma spectrum by separating the distinctive energy peaks, which can be problematic if a certain energy peak is not clear enough to be distinguished (Rider 2002).

Resistivity and SP logs are in principal a measurement of the electrical currents going through the wallrock. If these logs are used as a proxy for the lithology, it should be taken into account that they are also effected by the salinity of the porewater and the drilling fluid (Rider 2002). This makes the lithological interpretation of these well logs less straightforward and complicated, especially at the depths where the groundwater salinity is increasing more rapidly, which is often similar to the depth range of the Oosterhout Fm and Breda Sg (de Vries 2007).

5.2 Distribution of Glauconite

When all glauconite data from shallow wells in the Netherlands are assessed, it can be seen that while glauconite is found through the whole country, the highest glauconite content are often observed in the southern and eastern border regions (from Zeeland all the way to Groningen). In this regions, the density of the data from the Breda Sg and Oosterhout Fm is a lot higher than in the northwestern part of the Netherlands, because the top and base of the formations are more shallow in the border regions. Due to this data bias, it looks like the sediments in the northwest are less glauconitic in Figure 4-1a, while actually the wells just do not penetrate the more glauconitic Breda Sg and Oosterhout Fm. It should also be noted that several wells that do penetrate on the Breda Sg and/or the Oosterhout Fm, do not penetrate the formations fully. As a result, the highest glauconite content in the well can be less than it would have been if the deeper parts of the formations were included.

Even considering the differences in data density, the average glauconite content in the Oosterhout Fm decreases when you go in a NNW direction. In addition to the differences in depth between the eastern border regions and the northwest of the Netherlands, there also is a difference in thickness of the formations. In the regions where a higher glauconite content is observed is also the region where the former Breda Fm and Oosterhout Fm are very thin, which indicates that the average sedimentation rate in these formations has been lower here than in the ZZL and, for the Breda Fm, the RVG. As a low sedimentation rate is essential for glauconite evolution, it is probable that the high sedimentation rates in the areas where thicker deposits are found are the main cause for the low glauconite content observed.

In the Breda Sg, the pattern also is a correlation between the glauconite content and the amount of sand in the subgroup. The sandy part of the Breda Sg (Figure 2-5), has a similar regional distribution as the highly glauconitic lithologies (Figure 4-1 and 4-2). Apart from the fact that the glauconite minerals are much harder to observe in a clay layer, it can also be a result of the lower permeabilities of clay layers, that inhibit glauconite evolution by disconnecting the cations in the seawater from the glauconite grains in the subsurface.

Moreover, it is visible that the Breda Sg is in most wells more glauconitic than the Oosterhout Fm, with the exception of some wells in central Noord-Brabant where the Tilburg Mb had a higher glauconite content than the Breda Sg. Comparing the two formations is however difficult, as the lithological definition of the boundary between the formations is defined as a transitional decrease in shell content and an increase in glauconite content with depth. Thus, the Breda Sg is more glauconitic due to the lithostratigraphic definition used in the shallow well interpretation. It is thus probable that the upper part of the Breda Sg or Diessen Fm is interpreted where the lithology is more glauconitic, and not the other way around. This circular reasoning, together with the limited number of well data makes it hard to make a good interpretation of the vertical distribution of glauconite. Only when the formation boundaries are mostly based on shell content, biostratigraphy or seismic profiles, as is the case of the (revised) stratigraphy in the deep wells of Figure 4-6, the vertical distribution of glauconite within and between formations is truly independent of the interpretation. Therefore, the chronostratigraphic interpretation, that is still missing in a lot of wells, but is already done in the wells described by Houben (2025), is very useful for describing the distribution of glauconite and interpreting the GR.

To be able to interpret the formation boundaries independently in the lithostratigraphically interpreted shallow wells, the depth of the chronostratigraphic unconformities are evaluated (Figure 5-1). In the Kruisland (1) well B43E1411, the biostratigraphic interpretation of Houben (2025) is used. In the Kruisland (2) well B49E1470, Bergen op Zoom well B49E1446 and the Bemmel/Lingewaard well B40D2829+B40D2834, no biostratigraphic interpretation was available, but the likely depth of each unconformity could be derived from the GR log and preferably the glauconite independent U and Th logs, using the characteristics of the unconformities described by Munsterman et al. (2019). Considering the unconformities, the differences between the chronostratigraphic and lithostratigraphic interpretation become evident.

The alternative stratigraphic interpretation also leads to new insights into the vertical distribution of glauconite. Based on their position with respect to the three Miocene unconformities, three Glauconiet peaks are identified. The regional correlation of the identified peaks is shown in Figure 5-2.

1. The peak of the Tilburg Mb
   This glauconite peak is associated with the Tilburg Mb within the Oosterhout Fm, described by Munsterman et al. (2019). In the central part of Noord-Brabant, the peak is clearly visible as it is on top of the much less glauconitic Goirle Mb, such as in the Goirle well B50H0373 (Figure 4-4c) and well HVB-01 (Figure 4-6d and 5-3b). In other wells where the Goirle Mb is absent, the peak of the Tilburg Mb can still be found, whether or not less clearly. The glauconite peak is found just above the LMU in both the Bemmel/Lingewaard well B40D2829+B40D2834 and the JUT-01 well (Figure 5-2b). While less prominent, a small peak in glauconite content can also be observed just above the LMU in the Kruisland (2) well B49E1470 and the Bergen op Zoom well B49E1446 (Figure 5-2a).
2. The peak of the Diessen Fm
   This glauconite peak, found between the MMU and LMU, is best visible in the glauconite sands of the the Kruisland (2) well B49E1470 and the Bergen op Zoom well B49E1446 (Figure 5-2a). In the Kruisland (1) well B43E1411, the absence this glauconite peak can be explained by the absence of the Diessen Fm, as the LMU and MMU surfaces are directly on top of each other. This elevated glauconite content, although less extreme, is found in the upper part of the Diessen in both the Bemmel/Lingewaard well B40D2829+B40D2834 and the JUT-01 well (Figure 5-2b). In other wells, such as the HVB-01 well, the glauconite content gradually increases with depth in the Diessen Fm, and the peak of the Diessen Fm is found in the lower part of the formation (Figure 5-2b).

3. The peak of the Groote Heide Fm
   In the Groote Heide Fm, a glauconite peak is found in the three wells from Kruisland and Bergen op Zoom (Figure 5-2a). In these three wells, it is found relatively deeper within the formation when moving to the south. This is not unexpected, as lithological facies like the glauconitic sands are often synchronous due to changes in sea level and subsequent movement of the coastline. The Groote Heide glauconite peak is absent in all the deep wells as well as the Bemmel/Lingewaard well, where a small peak is found just below the EMU in the Veldhoven Fm instead (Figure 5-3b).

The different glauconite types, each linked to a different stage in the evolution process (Section 4.1.2). In the clay samples, the (highly) evolved stages were often not found. This is probably resulting from the low permeability of the sediments that reduce the interaction between the glauconite grains and the seawater. Therefore it is in line with expectations that the more evolved phases of glauconite are more often found in more permeable sand sediments. This is probably also the reason why the type 1 glauconite is more often found in finer sands of the peak of the Diessen Fm compared to the coarser sands in the peak of the Tilburg Mb.

The difference in glauconite evolution stage also means a difference in K content and consequently, the GR signal. It was not easy to quantify the abundance of the different types of glauconite grains in the samples, because the differences were quite subtle and often grains were in transition between the different stages. The most commonly found type was of the evolved stage, and therefore the K content of the evolved glauconite stage was used in the calculations of the glauconite effect on the GR and K log in the following sections.

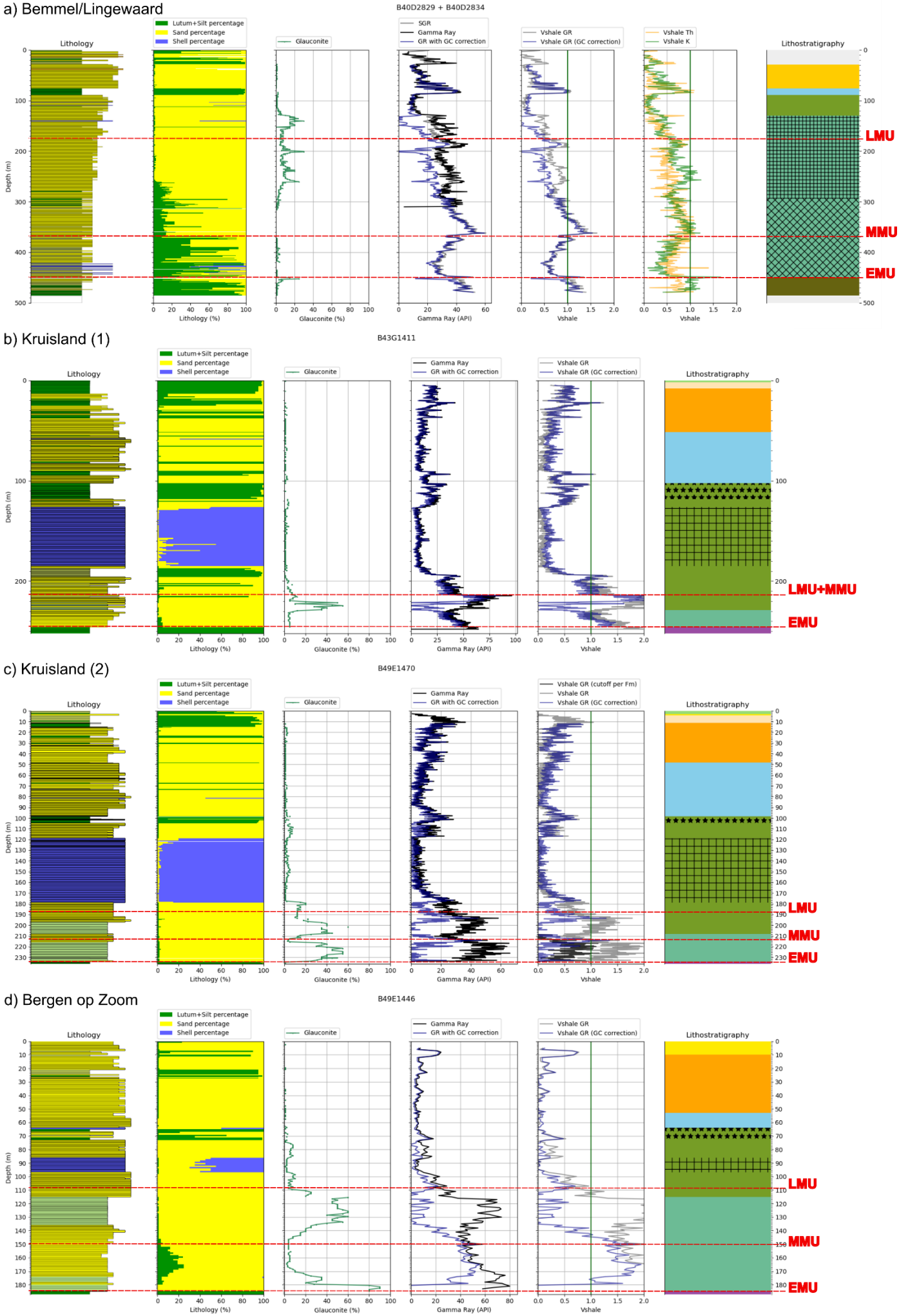

Figure 5-1: Lithology, glauconite content and lithostratigraphy, together with the GR, the glauconite-corrected GR and the results of the Vshale calculations of four shallow wells, including the interpreted Miocene unconformities.

a) Correlation of unconformities and glauconite peaks between Oranjeoord, Kruisland (1), Kruisland (2) and Bergen op Zoom

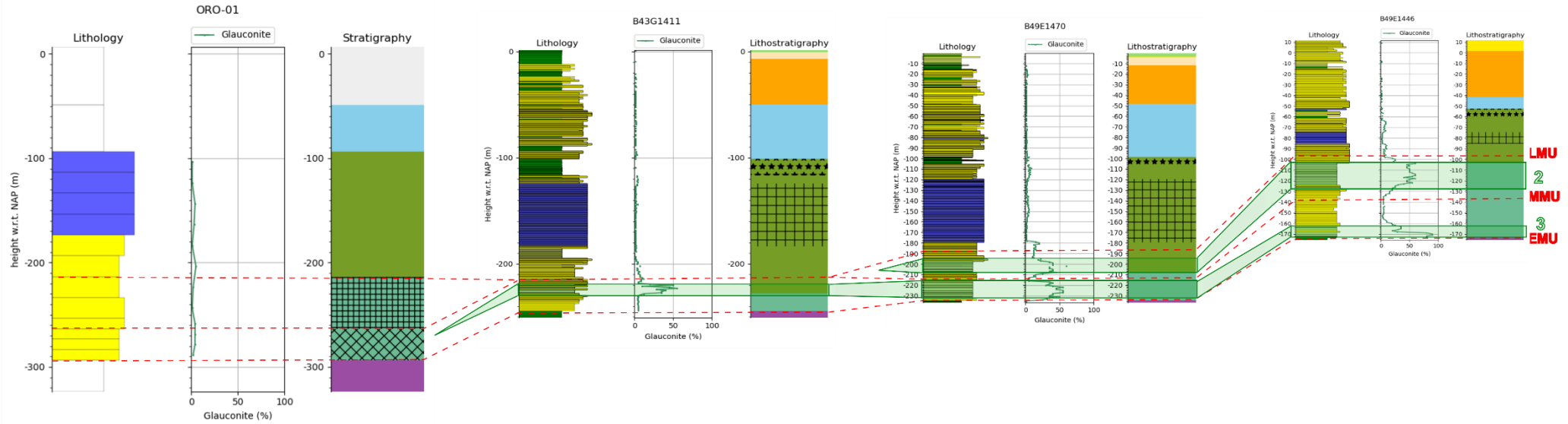

b) Correlation of unconformities and glauconite peaks between Amstelland, Jutphaas, Hilvarenbeek and Bemmel/Lingewaard

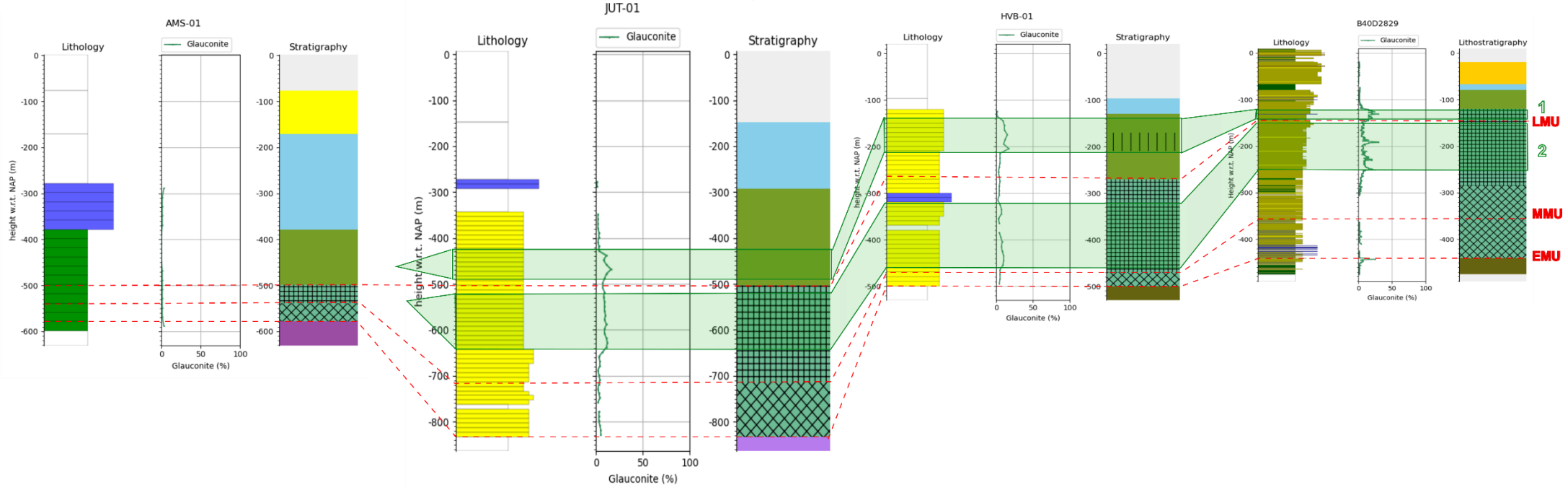

Figure 5-2: Correlation of the interpreted unconformities and the peaks in glauconite content from north to south for the western part of the WBR (a) and from west to east for the river area of the Netherlands, through both the ZZR and WBR. The numbers 1, 2 and 3 indicate the peak of the Tilburg Mb, the peak of the Diessen Fm and the peak of the Groote Heide Fm, respectively.

5.3 Recognising glauconite from SGR

5.3.1 Patterns in the SGR log

The K-enrichment in glauconite can be recognised with the SGR. When the SGR log is considered and compares to the glauconite content, it can be seen that most glauconite peaks are visible in the K signal. The pattern in the K-log in HVB-01 (Figure 4-6d), for instance, reflects the peak of the Tilburg Mb and the gradual increase with depth in the Diessen Fm. In the Bemmel/Lingewaard well B40D2829+B40D2834, the SGR-log also shows an increased K content at the same depths as glauconitic lithologies. Apart from some wells where glauconite was described with glauconite fraction classes, all glauconite peaks are accompanied with elevated K values.

However, the K peaks found in the SGR are not always accompanied with a peak in glauconite, such as the high K content in ORO-01 at 260-300m MD, the K peak in the Groote Heide Fm in HVB-01 or the peak in K content in the Bemmel/Lingewaard well at 360m MD. These 'non-glauconitic' K peaks can be explained in several ways. One option is that the glauconite content in the cutting is not representative of the wall rock. Especially in the deep wells ORO-01 and HVB-01, this is not unlikely, as really small bags of cutting material here represent 10m intervals. The washing process did not effect the cuttings too much, as the unwashed cuttings from ORO-01 showed no large difference in glauconite content in this interval. It could be that some glauconite breaks down in the drilling process, but even then the effect would be expected to be the same for the whole well, which is not the case at least in HVB-01, as many glauconite grains are found higherup in the stratigraphy. Another possibility is that the non-glauconitic K is really not glauconitic, but present in other minerals, such as illite, mica or feldspars. Muscovite micas were often found in these layers, but not in quantities that could explain such K peaks. Feldspars were not observed in the analysed cuttings and with the used methods it was not possible to identify whether the clay minerals are mostly illitic or of different mineralogy.

5.3.2 Th/K ratio

The Th-K mineral maps mostly reflect the same as the SGR logs. In the wells HVB-01 and Bemmel/Lingewaard, the more glauconitic lithologies clearly plot more towards the glauconite field. This trend is not seen in the ORO-01 well, because of the non-glauconitic K peak described above (Figure 4-6c). In the AMS-01 well, most data plots around the 'mixed layer clays' field, which reflects the observed lithology. In the Hank well B44E0146 and the Prinsenbeek well B44C0215, no relation is visible between lithology and the Th and K measurements. This is partly resulting from the glauconite fraction class data that is less precise and rather relative, thus making it harder to observe subtle differences in absolute glauconite content that relate to changes in Th and K content. The very low K values in the Prinsenbeek well are also influenced by the high shell content in the Oosterhout Fm, that results in a low GR values, meaning that Th/K ratios are more affected by background radiation and the chance of the Gamma radiation reaching the measuring tool.

It is not very surprising that lithologies with higher glauconite content are not always plotting in the glauconite field. The maximum glauconite content in these wells is 30% and often less, meaning that at least 70% of each lithology is non-glauconitic and has Th and K values that are more likely to plot in other fields. The SGR signal, resulting from mixed lithologies, are plotted on mineral maps that show the Th-K signal of theoretical end-member minerals. As a result, the Th-K not always plots in the field of the most dominant mineral, but rather shows a signal that is reflects a combination of many different minerals.

The mineral maps can also be used as way to quantify the change in Th/K ratio when lithologies get glauconitic, as is shown in Figure 5-4. As a theoretical highly glauconitic sediment is expected to plot in the glauconite field of the mineral map, a Th/K ratio of this theoretical end-member is expected to be between the coloured lines corresponding to a Th/K ratio of 0.6 and 1.5. The non-glauconitic end-member sediment can be more variable, depending on the sediment type, but is expected to plot in the 'mixed layer clay'/montmorillonite field and have an average Th/K ratio between 3.5 and 12, according to Rider (2002) and the non-glauconitic lithologies of the Bemmel/Lingewaard well shown on the Th-K mineral maps (Figure 4-8). This results in a theoretical relationship between Glauconite content and Th/K ratio. This relationship is expected not to be linear, but exponential, because the Th content is expected to be constant while the K content is affected by the glauconite. Thus, if the glauconite content rises from 1 to 2%, the amount of glauconitic K rises with factor 2, which has a much larger effect on the Th/K ratio than when the glauconite content rises from 20 to 21%, when the amount of glauconitic K rises with a factor of 1.05. This theoretical relationship, drawn in Figure 5-3, can prove to be useful in identifying glauconite-rich lithologies, but is not valuable when the effect of other radioactive minerals is more important or the Th/K ratio of the non-glauconitic end-member is different than that of a 'mixed layer clay'. This commonly occurs, as can be seen from the mineral maps of other wells in Figure 4-8. The theoretical relationship can of course be adjusted for a specific locality when it is used for comparison in follow-up research.

This theoretical relationship is tested and compared to the Th/K ratio measured in the wells, together with the results of Pauw and van Baak (2024) and an exponential trendline drawn through their results (Figure 5-4). In their research, they did XRD analysis to determine the glauconite content and did SGR measurements in the laboratory on the same samples. The samples are large bags of sediment from the Drongelen wells B44E1121 and B44E1124, and one sample from the Kattendijk Fm (the Belgian equivalent of the Oosterhout Fm) taken in the harbour of Antwerpen. They obtained a linear trendline from the 6 datapoints in their research, but instead, an exponential trendline is drawn through their datapoints in Figure 5-4, to compare it to the exponential the trends of the well data. The results of Pauw and van Baak (2024), as well as the trendline drawn through their data, fall within the theoretical boundaries of the Th/K-glauconite relationship. Some of the SGR measurements of ORO-01 fit the theoretical relationship, but other measurements in this well have very high Th/K ratios (up to 70 as is visible in Figure 4-9b), which cannot easily be explained by the lithological observations done. The AMS-01 and HVB-01 wells match better with the theoretical Th/K-glauconite relationship. Only the data of the Groote Heide Fm in HVB-01 has a lower Th/K ratio than expected, which is discussed in Section 4.2.1. In the plot of the Bemmel/Lingewaard well, it is observed that most data fit the theoretical boundaries, but some data around ca. 100m depth are more scattered and have higher and lower Th/K ratios than expected from the glauconite content. The lower Th/K ratios can be a result of the low K signal in shell-rich layers of the Oosterhout Fm. The higher Th/K ratio is measured in the peak of the Tilburg Mb at ca. 130-140m MD, where the K peak is lower than expected from the glauconite content in this interval.

The Th/K-glauconite relationship cannot be used to accurately quantify the amount of glauconite, but rather shows a range between theoretical end-members, between which the Th/K-glauconite relationship is expected to plot. The SGR is still a useful tool in identifying peaks in glauconite content, as the peaks in K-content, together with low Th/K ratios often indicate the presence of glauconitic lithologies. However, not every peak in the K log is related to glauconite and different minerals are expected to affect the SGR and GR logs too.

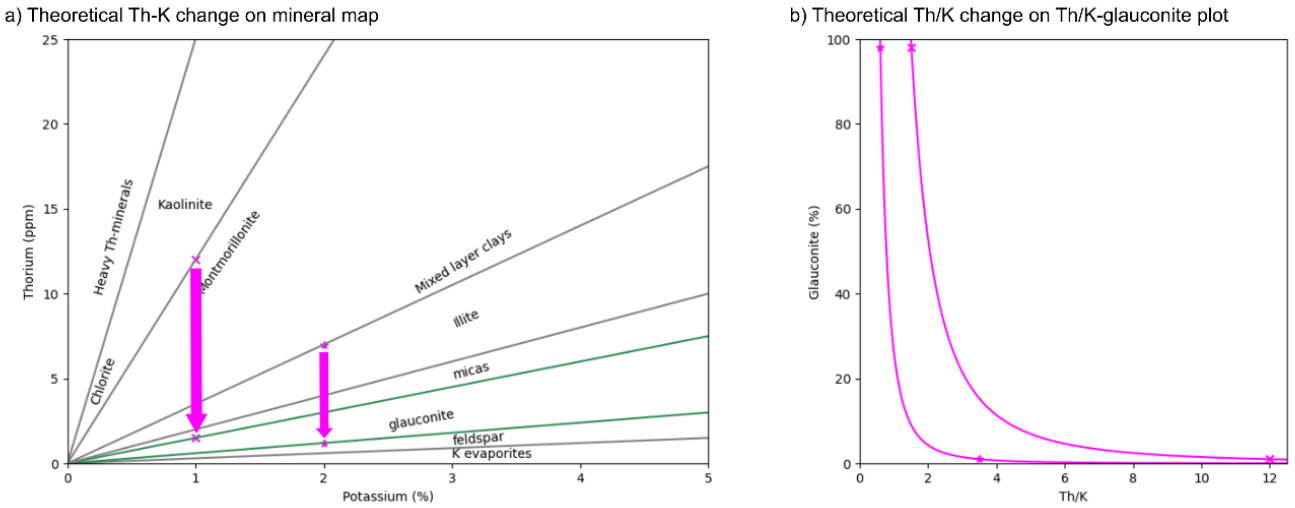

Figure 5-4: Theoretical change in Th/K ratio for different glauconite contents, shown by two arrows on the mineral map (a), that indicate the change from the assumed Th/K ratios two different clays to a glauconite-rich sediment. The arrows are translated to exponential lines between the two end-member values in the Th/K ratio against glauconite plot (b).

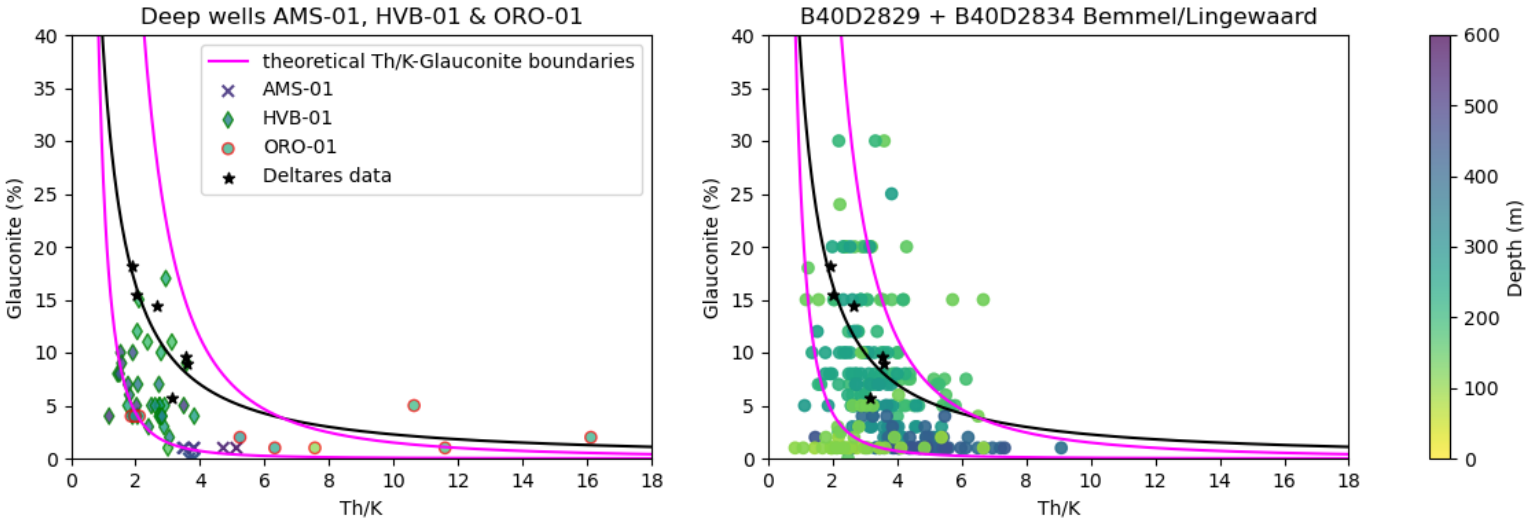

Figure 5-3: Glauconite content against Th/K ratio for the four deep wells AMS-01, HVB-01 and ORO-01 (left) and the Bemmel/Lingewaard well (right). In black the 'Deltares data' from the research by Pauw and van Baak (n.d.) is shown, including a exponential trendline plotted through their data. The Magenta line show the theoretical field in which the Th/K is expected to be for each glauconite content.

5.4 Unravelling the GR signal

To analyse and quantify the effect of glauconite on the GR, the mineralogy and SGR of the Bemmel/Lingewaard well B40D2829+B40D2834 is studied in more detail. The theoretical K-content and GR response of glauconite, muscovite and clay was compared to the SGR log (Figure 5-5). The calculation of the GR response of the minerals is described in Section 3.3, using the (semi-)quantitative observations of the mineral content. The calculated K content and GR signal of the minerals are shown with the cumulative coloured bars and then compared to the measured well logs.

From the figure, it can be seen that the response of the GR and K log in the upper 90m MD more or less reflects the lithology, as the peaks in GR and K coincide with the clay layers. The GR response of these shallow clays is mostly reflected by the Th log and, especially in the upper 50m, less by the K log. This is indicative of a more continental environment (Rider 2002).

The next peak in GR and K at 130m MD, does not reflect a clay layer, but a peak in glauconite content (the peak of the Tilburg Mb). The K response is however smaller than expected from the amount of (evolved) glauconite observed. Instead, a small increase in Th and U is observed here as well, which is more typical for other clay minerals. The glauconite observed here is mostly of type 2 and3, which are interpreted as (highly) evolved glauconite with high K contents. It could be that the low K content and higher U and Th content are the result of a darker little-evolved more smectitic/organic crust that forms around the grain in the evolved phase, as described by Piedrabuena (2024), which has more Th and U and less K. Below the LMU, the glauconite content, with a little muscovite as well, seems to be explaining the elevated K measured in these fine sands. This is, however, not enough to explain the complete GR signal, as some of the high GR is resulting from Th and U as well. A specific peak in Th and GR at ca. 180-190m is coinciding with a more goethite-rich lithological interval. Goethite is not necessarily radioactive by itself but is the most probable host for Th here, as no other observations can explain the Th peak. Lower in stratigraphy and closer to the MMU, the glauconite content decreases and the clay content slowly decreases. The GR signal rises further with depth, as well as the U, Th and K content. The slow increase in clay content and the mineralogy and lithology observed cannot explain this high GR response alone. While the peak in GR and specifically U is typical for the MMU, the grains or minerals that source of these radioactive elements are not known, as no increase in specific minerals or organic material is observed. It is characteristic for unconformities and lithologies with low sedimentation rate to be enriched in U, and possible sources can be organic material or phosphates (Rider 2002). Both are observed in the Breda Sg in this well and other wells, but no correlation between the abundance of these materials and the GR or SGR response is identified. This peak in the GR and U log is identified in many other wells at the depth of the MMU, such as the AMS-01, ORO-01 and HVB-01 well (Figure 4-6) and the Kruisland (1), Kruisland (2) and Bergen op Zoom well (Figure 4-3). This peak in uranium can also explain the depth difference between the GR peak and glauconite peak observed in the ADK-GT-01 well in the research of Smit (2022).

Below the MMU, the GR seems to more or less reflect the clay content again. The GR response in the deeper clays (>370m MD) is more reflected by the K signal, which indicates a more marine environment (Rider 2002). One short peak in GR and K, at the EMU, reflects not the clay content but a peak in glauconite.

In other wells, it can be seen that in the upper part of the Oosterhout Fm and the younger formations, the peak in the GR can be correlated to more shaly lithologies, as would be expected. In the deeper part of the Oosterhout Fm and the Breda Sg, this is not the case. High glauconite contents are reflected in the GR log here as well and often give even larger peaks that the clay layers. However, when a correction is applied for the presence of glauconite, there still are GR peaks left that cannot be explained by either the clay or the glauconite.

In the Kruisland (1) well B43E1411 for instance, until 200m MD, GR peaks of ca. 30-40 API indicate the presence of the clay layers. Form 200m MD to 220m MD the GR rises to a peak of 90 API, but no increase in clay or glauconite minerals is observed here. This exact peak in GR, together with the biostratigraphy, was used to identify the LMU+MMU at this depth (Houben 2025). At more or less the same depth of the GR peak, only a small peak of phosphate concretions is observed, which could hold high U concentrations in an unconformity (Rider 2002). A few meters below these unconformities the glauconite content increases and can explain most of the high GR signal here. In the lower part of the Breda Sg/ Groote Heide Fm, high GR values up to 50 API are still present where the glauconite content is lower. In the logs of the Kruisland (2) well B49E1470 and the Bergen op Zoom well B49E1446, it is also observed that some of the GR peaks in the Oosterhout Fm and Breda Sg can be explained by glauconite sands, but other elevated GR measurements cannot. Glauconite thus seems to be partly responsible for the elevated GR in these formations, but a significant amount of the GR response in these sands is not related to clay or glauconite.

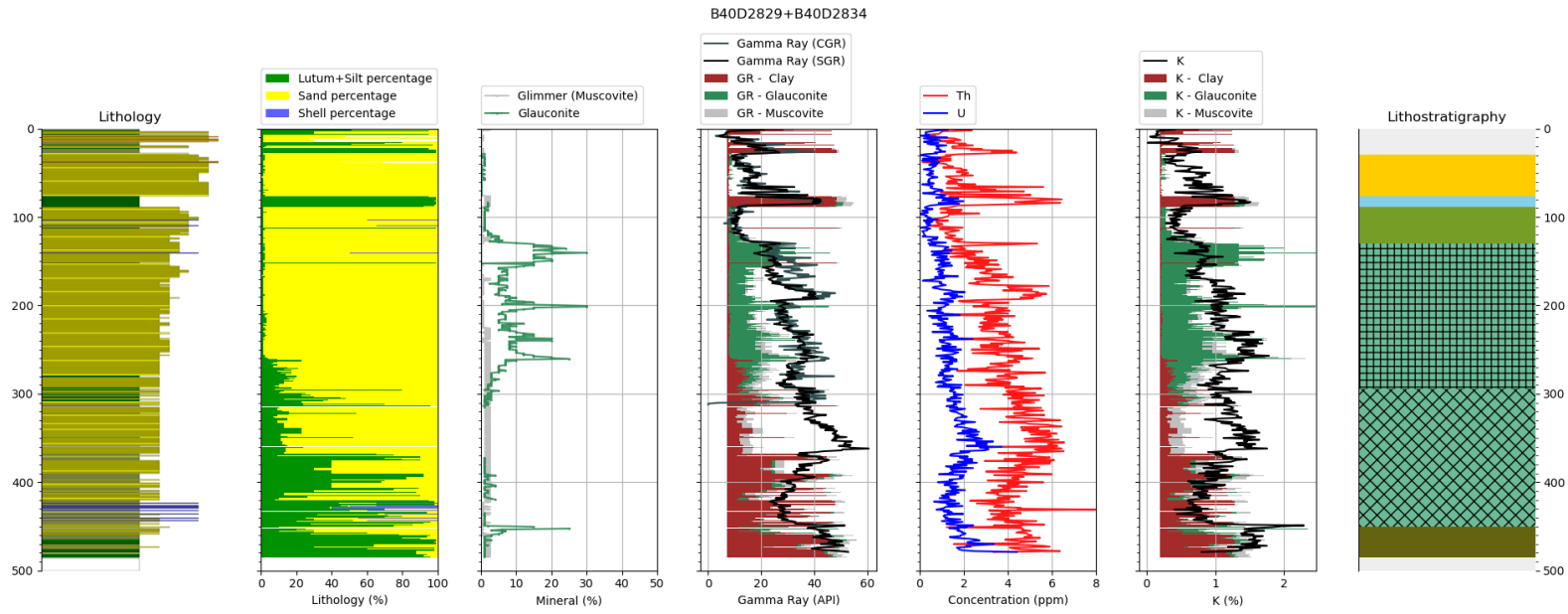

Figure 5-5: The Lithology, glauconite and mica content and lithostratigraphy of the Bemmel/Lingewaard well B40D2829+B40D2834, together with the GR and SGR. In the GR and K logs, the expected contributions of clay, glauconite and muscovite are shown, based on theoretical K, U and Th content and the lithological description.

5.5 Vshale interpretation

Different ways to calculate the Vshale from petrophysical well log were compared to each other and the observed lithology. The advantages and disadvantages of each method are listed below

1. Vshale from GR (not corrected)
   This is the most common method used to determine the Vshale in the subsurface. For the Breda Sg and lower part of the Oosterhout Fm, this Vshale alone can lead to misinterpretation. Even when the shale and sand cutoffs are redetermined for each formation, as is usually done, the Vshale does not always truly reflect the lithology. The interpretation with different cutoffs for each formation can clearly help to decrease the mismatch of the Vshale, especially when the glauconite content and elevated U (and Th) levels are rather constant within a formation. For variations in glauconite content within one formation, such as in the Breda Sg of Bergen op Zoom B49E1446, or local peaks in U, such as at the MMU, calculating the Vshale for each separate formation is not sufficient to exclude all unwanted effect. Therefore, if the Vshale from GR is used on the Oosterhout Fm and Breda Sg, it should be compared to other petrophysical logs as well and mistrusted if a significant difference between the Vshales of two different logging methods is observed. Moreover, to identify the U-rich unconformities and clearly define boundaries of formations, that are useful for interpreting each separate formation, biostratigraphical analysis is also important to decrease the mismatch of the Vshale.
2. Vshale from GR (GC correction)
   When the GR is corrected for a theoretical response of glauconitic sands, the part of the shale-peaks that actually reflect glauconite sands are removed. Unfortunately, this seems to be not the only problem in misinterpreting the Vshale in the Oosterhout Fm and Breda Sg. Especially sediments with elevated Th and U concentration, mainly around the Miocene unconformities, influence the GR log and Vshale often even more than glauconite. Moreover this correction can only be applied when there is detailed information about the glauconite content in a well, which is often not the case for the wells where the Vshale calculation form petrophysical well logs is most useful.
3. Vshale from SGR (U, Th and K) log
   A Vshale can also be calculated for the U, Th and K signal separately. Of these logs, a Vshale from U seems to reflect more the unconformities than the shale layers. The Vshale from K is not affected as much by the unconformities. However, the Vshale from K reflects elevated glauconite content as much as it reflects clay layers and is therefore not a good method to identify shales only. The Vshale from the Th log is theoretically not effected by the unconformities and the glauconitic lithologies. This is visible in the calculated Vshales as well, although some elevated Th values are observed around unconformities. The Th log does sometimes show a shale response in a sandy lithology, such as the goethite interval at 180-190m MD in the Bemmel/Lingewaard well, but is the most reliable of the three radioactive elements in the Vshale interpretation. The best way to use the SGR for identifying shale layers is by looking at all three elements, because shales and clay lithologies show an increase in U, Th and K most of the time, while and abundance of accessory minerals are often only seen in one or two of the radioactive element logs.

4. Vshale from SP or resitivity log
   Calculating a Vshale from the SP log is already more complex, but very useful for calibration and comparison of the GR Vshale. The Vshale from SP often indicates clearly where more shaly lithologies are present and is unaffected by unconformities and accessory minerals such as glauconite. The SP log is affected by changes in groundwater salinity. As the Breda Sg is often at a depth where groundwater gets more saline, it is therefore sometimes hard to interpret the Vshale correctly from the SP log. Another downside of the SP log is that it cannot be used offshore. The resistivity log also shown peaks and deviations that indicate shale layers in a more qualitative than quantitative manner. A shale response in a GR log can thus be tested to see if it is also visible in a resistivity lo, indicating that it probably is a true shale. The resistivity, however, is also affected by groundwater salinity and cannot be used for quantitative Vshale computations.
5. Vshale from other petrophysical logs
   There are more well logs that can be used for Vshale computations, such as Neutron-Density and Nuclear Magnetic Resonance. These well logs are less commonly measured in Dutch wells, but could prove to be useful as they are less effected by accessory minerals. The NMR can for instance be corrected for the presence of glauconite (Abouzaid et al. 2016). The Vshale from the ND log in well ORO-01 (Figure 4-9c) seemed to be in line with the Vshale from the Th log, except for shale peaks at the unconformities. These, and Vshale computations from other petrophysical well logs, were not further analysed as this was beyond the scope of the project.

In general, there are a lot of possibilities for obtaining a reliable lithology interpretation from petrophysical well logs. Every well log has its own advantages and disadvantages, that contribute to their reliability, especially in the rather complex Breda Sg. A combination of multiple well log interpretations is preferred, as this improves the understanding of the lithology and helps to identify the flaws in the separate well log interpretations. The SP log is a very useful tool to use for calibrating and comparing the GR log, if one takes into account its limitations. If the GR log is used for interpreting the lithology in the Breda Sg and lower Oosterhout Fm, the SGR is crucial in understanding the source of the GR signal and distinguishing the GR response of clay, K-rich glauconite, U-enriched unconformities and other accessory minerals contributing to the enrichment in specific radioactive elements.

6 Conclusion

6.1 Conclusions

The outcomes of this research help improve to understand the glauconite in the Oosterhout Fm and Breda Sg and have shed light on the problematic interpretation of the GR. In addition, the research helps to assess the risks of other practices that can be affected by the presence of glauconite, including pile driving and drilling operations. The main conclusions of this research are summed up below as answers to the four research questions.

- What is the presence and distribution of glauconite in the Oosterhout Formation and Breda Subgroup of the Upper North Sea group in the research areas?

Laterally, glauconite occurs almost everywhere in the Dutch subsurface and is often found in formations with a shallow marine origin. Both vertically and laterally, the glauconite content can vary from 1% up to 90%, and the highest glauconite content are found in the Vaals Fm in southern Limburg and the Oosterhout Fm and Breda Sg in the rest of the Netherlands.

Within the Oosterhout Fm and Breda Sg, the highest glauconite content is found in the southern, eastern and central parts of the country. The glauconite content is low in wells from Noord-Holland and Zuid-Holland, where the Breda Sg is clay-dominated. The three identified peaks in glauconite content are, from young and shallow to old and deep: The peak of the Tilburg Mb in the Oosterhout Fm), the peak of the Diessen Fm (between the LMU and MMU) and the peak of the Groote Heide Fm (between the MMU and EMU). In the research area, the peak of the Tilburg Mb is present in the eatern part of the WBR and the southeast of the ZZR. The peak of the Diessen Fm is present in almost the whole WBR and ZZR, with the exception of the northwest of the regions, where the Diessen Fm is not sand but clay dominated. The peak of the Groote Heide Fm is best visible in the west of the WBR, but can be found in most of the WBR. In the ZZR, this peak was not found in the few wells that reached the depths of the Groote Heide Fm.

In the research areas, glauconite is found in all stages of glauconite evolution, but most of the glauconite is in the evolved stage. Differences in the appearance of the glauconite and the (relative) amount of (highly) evolved glauconite can possibly be linked to differences in grain size, porosity and permeability.

- Can glauconitic lithologies be identified using spectral gamma ray logs?

SGR logs are a useful tool to enhance the understanding of the GR signal in the Oosterhout Fm and Breda Sg. Lithologies with high glauconite content can often be identified by a peak in K only, while clay intervals have elevated K, Th and U values. The SGR also helps to identify other accessory minerals or other GR peaks that are not clay related, such as the peak in U that is often found at the MMU. While the Th/K ratio of lithologies is related to the glauconite content in a theoretically expected exponential manner, the range of uncertainty within the theoretical boundaries is too large to be used as reliable quantitative method to estimate the glauconite content in a lithology. The Th/K ratio can help to qualitatively identify glauconitic lithologies.

- How large is the impact of glauconite on the gamma ray log?

The impact of glauconite on the GR log is mainly resulting from the K-content of the glauconite (varying with evolutionary stage) and the amount of glauconite in the lithology. When the GR is corrected for the theoretical effect of glauconite, it is observed that a glauconite content of more than ca. 5% has a significant effect on the GR, which is increasing further with increasing glauconite content. While a glauconite content can explain a number of the GR peaks, there are also a lot of GR peaks that are not related to either glauconite or clay. In almost every well, increased U content is measured around the Miocene unconformities, mainly the MMU. A Th peak was found in the Bemmel/Lingewaard well, but not in many other wells. Furthermore, the U and Th values are generally higher too in the Breda Sg, contributing to the higher GR values. Thus, while the impact of glauconite on the GR is significant, it is not the most dominant contributor to the elevated GR values per se.

- Which alternative methods or corrections for the effect of glauconite can improve the interpretation of petrophysical well logs?

To improve the Vshale interpretation from petrophysical well logs, the most important is to compare the GR log to lithological or other petrophysical logs. When the lithology is described in detail, a correction can be applied that corrects for the glauconite content, solving a part of the problem in the interpretation. The SGR log is helpful in understanding the different contributors to the GR signal and can be used to calculate the Vshale from the Th log, that is less effected by glauconite and unconformities. When there is less lithological data available, it is also important to use the Resistivity log and the Vshale calculated with SP and ND logs, to calibrate and compare the Vshale from GR to separate true shale intervals from other glauconite of unconformity related peaks in the GR.

6.2 Recommendations

While this research is an enlightening exploration of the problems in the Oosterhout Fm and Breda Sg, it is only a first step in understanding the complexities of these formations. One of the main takeaways of this research is that improving the interpretation of the petrophysical well logs in the Oosterhout Fm and Breda Sg, and understanding the impact of the glauconite completely are still a work in progress. The rather limited understanding of these formations, compared to shallower and deeper parts of the subsurface, provides a number of challenges in the lithological characterisation that is of essential for geothermal exploration and ATES in these formations. Recommendations to further improve the understanding of these formations are listed below.

- To be able to optimally describe variations within the Breda Sg, the new stratigraphical definition of the Breda Sg should be further extrapolated to provide a better framework in which the variations in glauconite content can be described and Vshale cutoffs can be adjusted for more constantly elevated GR values. Mapping the Miocene unconformities also helps to identify the unconformity-related elevated GR values in the Breda Sg and distinguish them from clay lithologies.
- The lithostratigraphic interpretation of the Breda Sg can be used to identify the first increase of glauconite content with depth, as increased glauconite content is one of the characteristics used to define the top of the Breda.
- To better understand lateral variation in the glauconite content in the Netherlands, including areas with relatively high ATES and geothermal potential, it is important to increase the data density of the Breda Sg in the provinces of Utrecht, Flevoland, Noord-Holland and Zuid-Holland. This can be done by drilling new wells with high resolution lithological sampling, preferably by coring, and in the Oosterhout Fm and Breda Sg, which are also analysed by a SGR log and potentially a SP log.

- Cuttings and petrophysical well logs of deep NLOG wells, especially those located in the area where the Oosterhout Fm and Breda Sg are deeper than 500m, should be analysed and described in more detail to improve the available quantitative data on lithology and glauconite content, with the same methods that are used for shallow wells on Dinoloket.
- In further research the uncertainties of glauconite data from especially older wells should be taken into account, and a study can be done to determine whether the glauconite fraction classification that is derived from the written well descriptions truly represents the percentage range given by Bosch (2000).
- Follow-up research can attempt to achieve a method to quantitatively estimate the glauconite content from the SGR or other methods, but the uncertainty in the relationship between glauconite content and the Th/K ratio is too high to provide a precise estimate.
- In future petrophysical analyses, the Vshale log can be improved by using the SGR, resistivity and SP to distinguish true shale signals from those reflecting accessory minerals like glauconite. In general, true shales are often reflected by a peak in all three radioactive elements of the SGR and a shift in Resistivity and SP values. Glauconitic sands are often only reflected by increased K values and unconformities, especially the MMU, are often mainly reflected by a peak in U.

7 Acknowledgements

This research is part of the Warmig^{UP}*GOO* project, made possible by the subsidies from the 'Rijksdienst voor Ondernemend Nederland' (RVO), within the subsidy scheme 'Missiegedreven Onderzoek, Ontwikkeling en Innovatie' (MOOI), for RVO known under the project number 'MOOI322012'.

I would like to thank my main supervisors, Lies Peters, Angela Pascarella and Sonja Geilert for guiding me in this project and brainstorming with me about all the results and their implications. Moreover I would like to thank TNO for the opportunity to contribute to this project and get to know the company. Further, I would like to thank Chris van Baak, Pieter Pauw and Tommer Vermaas of Deltares for the useful discussions we shared, the insights and results they provided and the opportunity to use the Deltares laboratory facilities. I would like to thank the colleagues working at the Core Shed and the Description Area for helping me with providing the material and facilities for the cutting analysis, with special thanks to Nico Janssen and Hein van Mulligen, who helped me in getting familiar with the lithological description methods, recognising different minerals and using the microscope and camera. Furthermore, I am grateful for the data and help with handling the large datasets I received from Hans Veldkamp, Zanne Korevaar and Stefanie Bus. At last I want to acknowledge all colleagues of TNO-GDN, and especially from the Geohydrology team, who welcomed me with open arms and were always available to answer my questions.

8 Bibliography

Abouzaid, Ahmed, Holger Thern, Mohamed Said, Mohammad ElSaqqa, Mohamed Elbastawesy, and Sherin Ghozlan. 2016. 'Nuclear Magnetic Resonance Logging While Drilling in Complex Lithology – Solution for a Glauconitic Sandstone Reservoir'. In *All Days*, SPE-AFRC-2579089-MS. Nairobi City, Kenya: SPE. https://doi.org/10.2118/AFRC-2579089-MS.

Adriaens, R., N. Vandenberghe, and J. Elsen. 2014. 'Natural Clay-Sized Glauconite in the Neogene Deposits of the Campine Basin (Belgium)'. *Clays and Clay Minerals* 62 (1): 35–52. https://doi.org/10.1346/CCMN.2014.0620104.

Amorosi, Alessandro, Irene Sammartino, and Fabio Tateo. 2007. 'Evolution Patterns of Glaucony Maturity: A Mineralogical and Geochemical Approach'. *Deep Sea Research Part II: Topical Studies in Oceanography*, Authigenic Mineral Formation in the Marine Environment; Pathways, Processes and Products, 54 (11): 1364–74. https://doi.org/10.1016/j.dsr2.2007.04.006.

Baldermann, Andre, Laurence N. Warr, Georg H. Grathoff, and Martin Dietzel. 2013. 'THE RATE AND MECHANISM OF DEEP-SEA GLAUCONITE FORMATION AT THE IVORY COAST–GHANA MARGINAL RIDGE'. *Clays and Clay Minerals* 61 (3): 258–76. https://doi.org/10.1346/CCMN.2013.0610307.

Bosch, J.H.A. 2000. 'Standaard Boor Beschrijvingsmethode'. 00-141-A 00-141-A. TNO-NITG.

Diaz, E, M Prasad, M A Gutierrez, and J Dvorkin. 2002. 'Effect of Glauconite on the Elastic Properties, Porosity, and Permeability of Reservoirs Rocks'.

Drits, V. A., T. A. Ivanovskaya, B. A. Sakharov, B. B. Zvyagina, A. Derkowski, N. V. Gor'kova, E. V. Pokrovskaya, A. T. Savichev, and T. S. Zaitseva. 2010. 'Nature of the Structural and Crystal-Chemical Heterogeneity of the Mg-Rich Glauconite (Riphean, Anabar Uplift)'. *Lithology and Mineral Resources* 45 (6): 555–76. https://doi.org/10.1134/S0024490210060040.

Houben, A J P. 2025. 'Biostratigraphy of Miocene Strata in the Netherlands'. WarimgUP. TNO. https://www.warmingup.info/resultaten.

Houben, A J P, Z. Korevaar, C. Heerema, E. Peters, and E. De Boever. 2023. 'Data inventory for the improvement of Upper North Sea group geological models'. TNO.

Huff, Warren. 1990. 'X-Ray Diffraction and the Identification and Analysis of Clay Minerals'. *Clays and Clay Minerals* 38 (January):448–448. https://doi.org/10.1346/CCMN.1990.0380416.

Korevaar, Z E R (Zanne). 2023. 'Designing an Experimental Set-up for Measuring Thermal Conductivity of Sediments'.

Li, Xiang, Yuanfeng Cai, Xiumian Hu, Zhicheng Huang, and Jiangang Wang. 2012. 'Mineralogical Characteristics and Geological Significance of Albian (Early Cretaceous) Glauconite in Zanda, Southwestern Tibet, China'. *Clay Minerals* 47 (1): 45–58. https://doi.org/10.1180/claymin.2012.047.1.45.

López-Quirós, Adrián, Carlota Escutia, Antonio Sánchez-Navas, Fernando Nieto, Antonio Garcia-Casco, Agustín Martín-Algarra, Dimitris Evangelinos, and Ariadna Salabarnada. 2019. 'Glaucony Authigenesis, Maturity and Alteration in the Weddell Sea: An Indicator of Paleoenvironmental Conditions before the Onset of Antarctic Glaciation'. *Scientific Reports* 9 (1): 13580. https://doi.org/10.1038/s41598-019-50107-1.

López-Quirós, Adrián, Antonio Sánchez-Navas, Fernando Nieto, and Carlota Escutia. 2020. 'New Insights into the Nature of Glauconite'. *American Mineralogist* 105 (5): 674–86. https://doi.org/10.2138/am-2020-7341.

Munsterman, Dirk K., T.H. Donders, A.J.P. Houben, J.H. Ten Veen, and F.P. Wesselingh. 2025. 'Paleogene-Neogene'. In *J. H. Ten Veen, G. J. Vis, J. De Jager, & Th. E. Wong (Eds.), Geology of the Netherlands, Second Edition* . Amsterdam University Press.
Munsterman, Dirk K., Johan H. Ten Veen, Armin Menkovic, Jef Deckers, Nora Witmans, Jasper Verhaegen, Susan J. Kerstholt-Boegehold, Tamara Van De Ven, and Freek S. Busschers. 2019. 'An Updated and Revised Stratigraphic Framework for the Miocene and Earliest Pliocene Strata of the Roer Valley Graben and Adjacent Blocks'. *Netherlands Journal of Geosciences* 98:e8. https://doi.org/10.1017/njg.2019.10.
Nichols, Gary. 2009. *Sedimentology and Stratigraphy*. Second Edition. John Wiley & Sons Ltd.
Obasi, Christian C., Dennis O. Terry Jr., George H. Myer, and David E. Grandstaff. 2011. 'Glauconite Composition and Morphology, Shocked Quartz, and the Origin of the Cretaceous(?) Main Fossiliferous Layer (MFL) in Southern New Jersey, U.S.A.' *Journal of Sedimentary Research* 81 (7): 479–94. https://doi.org/10.2110/jsr.2011.42.
Odin, G. S., and Albert Matter. 1981. 'De Glauconiarum Origine'. *Sedimentology* 28 (5): 611–41. https://doi.org/10.1111/j.1365-3091.1981.tb01925.x.
Patchett, J G, R Wiley, and Mostafa El Bahr. 1993. 'MODELING THE EFFECTS OF GLAUCONITE ON SOME OPENHOLE LOGS FROM THE LOWER SENONIAN IN EGYPT'.
Pauw, P., and C.G.C. van Baak. 2024. 'Karakterisatie van glauconiethoudende, Tertiaire afzettingen in Nederland voor verbeterde ondergrondse opslag van water en energie'. Concept Deltares report.
Peters, E, J P T Foeken, C R Geel, and J G Veldkamp. 2022. 'Characterization of and Production from the Breda Formation in the Roer Valley Graben'. WarmingUP. TNO. https://www.warmingup.info/resultaten.
Piedrabuena, Alba Rodríguez. 2024. 'First Steps into the Calibration Chamber Pile Tests with Glauconitic Sands'. Delft University of Technology.
Rider, Malcolm. 2002. *The Geological Interpretation Of Well Logs*. Second Edition. Sutherland, Scotland: Rider-French Consulting Ltd.
Rieder, Milan, Giancarlo Cavazzini, Yurii S. D'yakonov, Viktor A. Frank-Kamenetskii, Glauco Gottardi, Stephen Guggenheim, Pavel W. Koval', et al. 1998. 'Nomenclature of the Micas'. *Clays and Clay Minerals* 46 (5): 586–95. https://doi.org/10.1346/CCMN.1998.0460513.
Schlumberger. 2013. *Log Interpretation Charts*. 2013th ed.
Serra, Oberto. 1984. *Fundamentals of Well-Log Interpretation*. Developments in Petroleum Science 15A-15B. Amsterdam New York Pau: Elsevier Elf Aquitaine.
Smit, Freek. 2022. 'An Overlooked Aquifer in the Netherlands: Geothermal Potential of the Breda Formation in the Zuiderzee Low'.
Staveren, M. Th. van, and J.M. de Wit. 1995. 'Westerschelde Oeververbinding; Geotechnische Opinie Glauconitehoudende Zanden (Zanden van Berg, Formaties van Breda En Oosterhout)'. CO-350690/371. Delft: Grondmechanica Delft.
Thomas, Wibeke Hammervold, Jon Knut Ringen, Sten Ola Rasch, and Statoil Asa. 2003. 'Effect of Glauconite on Petrophysical Properties as Revealed by Core Analysis'. In . Pau, France.
TNO-GDN. 2024a. 'Formatie van Breda'. Stratigrafische Nomenclator van Nederland , TNO – Geologische Dienst Nederland. 2024. https://www.dinoloket.nl/stratigrafische-nomenclator/formatie-van-breda.
———. 2024b. 'Formatie van Oosterhout'. Stratigrafische Nomenclator van Nederland , TNO – Geologische Dienst Nederland. 2024. https://www.dinoloket.nl/stratigrafische-nomenclator/formatie-van-oosterhout.
———. 2025a. 'Dinoloket'. Dinoloket. 2025. https://www.dinoloket.nl/.
———. 2025b. 'NLOG'. Nederlands Olie- En Gasportaal. 2025. https://www.nlog.nl/.
———. 2025c. 'Upper North Sea Group'. Nomenclature of the Netherlands, TNO – Geological Survey of the Netherlands. 2025. https://www.dinoloket.nl/en/stratigraphic-nomenclature/upper-north-sea-group.

Van Alboom, Gauthier, Hilde Dupont, Jan Maertens, and Koen Haeltema. 2012. 'Glauconiethoudende Zanden'. *Geotechniek*, April, 32–37.
VANCAMP, Alexander. 2011. 'GRONDMECHANISCHE HERKENNING EN EIGENSCHAPPEN VAN GLAUCONIETZANDEN'.
Vandenberghe, Noël, W. Burleigh Harris, J. M. Wampler, Rik Houthuys, Stephen Louwye, Rieko Adriaens, Koen Vos, et al. 2014. 'The Implications of K-Ar Glauconite Dating of the Diest Formation on the Paleogeography of the Upper Miocene in Belgium'. *GEOLOGICA BELGICA* 17 (2): 161–74. http://hdl.handle.net/1854/LU-5784605.
Veldkamp, J. G., C. R. Geel, and E. Peters. 2022. 'Characterization of Aquifer Properties of the Brussels Sand Member from Cuttings'. WarmingUP. TNO. https://www.warmingup.info/resultaten.
Veldkamp, J. G., E Peters, J Foeken, F Smit, and K Geel. 2023. 'Breda Formation – Target for Shallow Geothermal Exploration'. Presented at the European Geothermal Workshop, November. https://www.warmingup.info/resultaten.
Vries, J.J. de. 2007. 'Groundwater'. In *Th.E. Wong, D.A.J. Batjes & J. de Jager, Geology of the Netherlands*, 295–315. Royal Netherlands Academy of Arts and Sciences.
Vrijlandt, M., D. Dinkelman, G.J. Otero Rodriguez, and M. Koenen. 2023. 'National High Temperature Aquifer Thermal Energy Storage Potential Tool'. WarmingUP. TNO. https://www.warmingup.info/resultaten.
Westgate, Zachary J., Don J. DeGroot, Christopher McMullin, Yuanjing Zou, Dongdong Guo, Simon Van Haren, Ryan D. Beemer, Danilo Zeppilli, Kenneth G. Miller, and James V. Browning. 2023. 'Effect of Degradation on Geotechnical Behavior of Glauconite Sands from the U.S. Mid-Atlantic Coastal Plain'. *Ocean Engineering* 283 (September):115081. https://doi.org/10.1016/j.oceaneng.2023.115081.

Appendix A: Nomenclature

Abbreviation	Full phrase
ATES	Aquifer Thermal Energy Storage
Cal	Caliper log
Fm	Formation
GR	Gamma Ray log
Mb	Member
ND	Neutron and Density log (interpreted together)
NLOG	Nederlands Olie- en Gasportaal
NMR	Nuclear Magnetic Resonance log
RVG	Roer Valley Graben
Sg	Subgroup
SGR	Spectral Gamma Ray
SP	Spontaneous Potential
Warming^{UP}*GOO*	Warming^{UP} Geothermal and Storage Upscaling
ZZL	Zuiderzee Low

Symbol	Description	Unit
GR	Gamma Ray Signal	API/GAPI
K	Potassium content	Mass percentage (%)
LNR	Long normal resistivity	Ohm meter ($\Omega \cdot \mathrm{m}$)
M_L	Fraction of a mineral in a lithological unit	-
RES	Resistivity	Ohm meter ($\Omega \cdot \mathrm{m}$)
SNR	Short normal resistivity	Ohm meter ($\Omega \cdot \mathrm{m}$)
SP	Spontaneous potential	Millivolts (mV)
Th	Thorium content	Parts per million (ppm)
Th/K	Thorium/potassium ratio	Part per million/mass percentage (ppm/%)
U	Uranium content	Parts per million (ppm)
$Vshale$	Volume of Shale, an indication of clay mineral fraction in a lithological unit	-
X_M	Fraction of a element within a mineral	-

Appendix B: Legend of lithology and stratigraphy

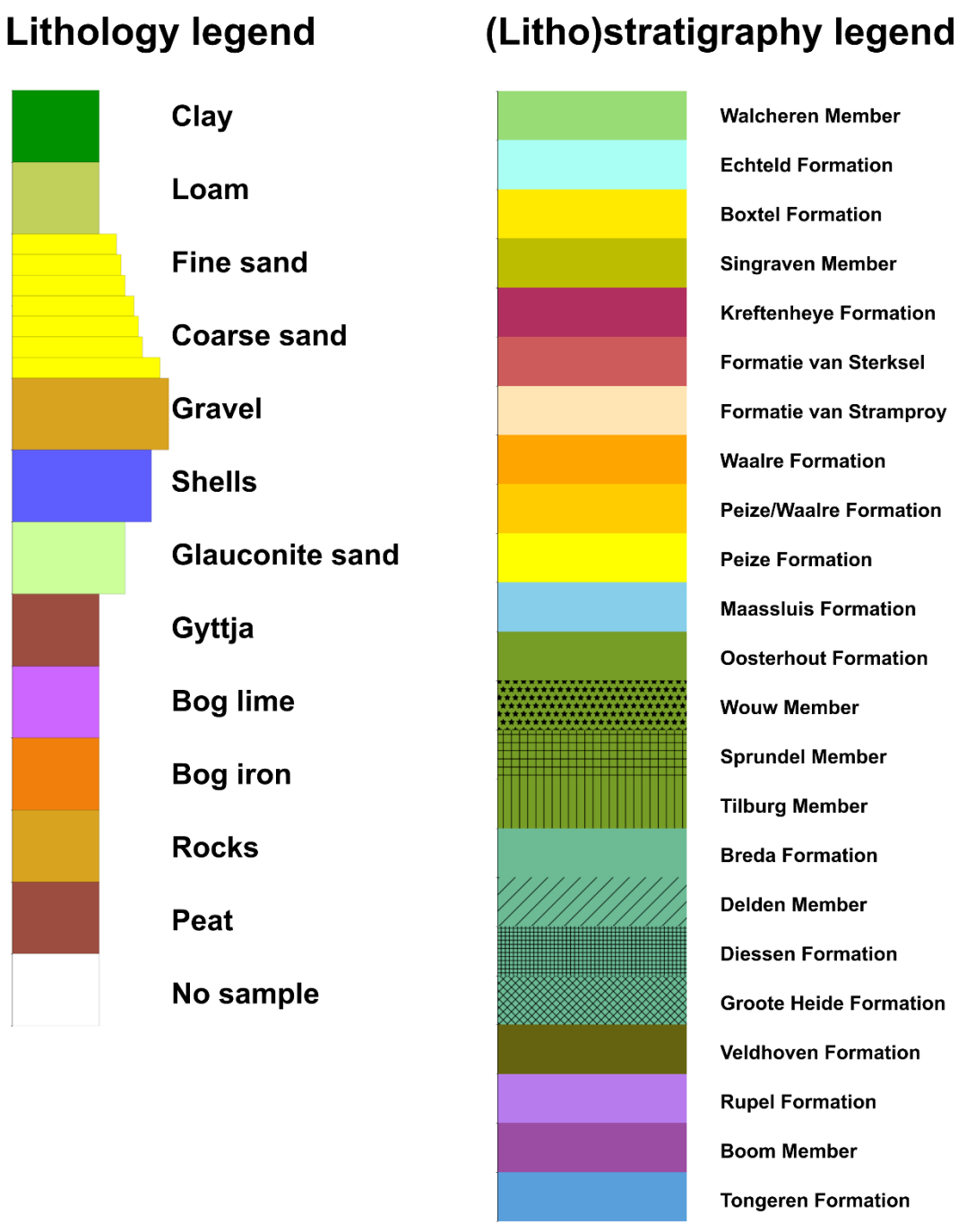

Appendix C: Chart for visual estimation